*nutrients*

MDPI

*Systematic Review*

# A Systematic Review of Neuroimaging Evidence on Human Milk Oligosaccharides and Neurodevelopment: Brain Structure, Metabolism, Mechanistic Insights, and Future Directions

**Md Mahmudul Amin [1,2], Tanjina Amin [1,2], Adikari Arachchige Dilki Indrachapa Adikari [1], Xiaoming Zheng [3], Zhongkai Zhou [1,4] and Bing Wang [1,*]**

[1] School of Agricultural, Environmental and Veterinary Sciences, Charles Sturt University, Wagga Wagga, NSW 2678, Australia; mdamin@csu.edu.au (M.M.A.); tamin@csu.edu.au (T.A.); dadikariarachchige@csu.edu.au (A.A.D.I.A.); zzhou@csu.edu.au (Z.Z.)
[2] Department of Anatomy and Histology, Faculty of Veterinary Medicine and Animal Science, Gazipur Agricultural University, Gazipur 1706, Bangladesh
[3] School of Dentistry and Medical Sciences, Charles Sturt University, Wagga Wagga, NSW 2678, Australia; xzheng@csu.edu.au
[4] College of Food Science, Southwest University, Chongqing 400715, China
* Correspondence: biwang@csu.edu.au

## Abstract

Background/Objectives: Human milk oligosaccharides (HMOs) are bioactive glycans that may influence neurodevelopment through microbiota-dependent and independent pathways. This systematic review critically evaluates neuroimaging evidence linking HMO exposure to brain structure, microstructural organization, and neurochemical profiles, integrating imaging-derived outcomes with proposed molecular mechanisms and assessing their translational relevance to human infants. Methods: PubMed, MEDLINE, and Scopus were systematically searched from database inception to November 2026 for human and animal intervention studies investigating HMO-associated neuroimaging outcomes. Evidence was narratively synthesized according to HMO composition, dosage, developmental stage, imaging modality, and methodological quality. Results: Eight eligible intervention studies were identified, all involving neonatal piglets; no human intervention studies met the neuroimaging eligibility criteria. Magnetic resonance spectroscopy findings suggested that sialylated HMO formulations were associated with positive changes in selected cerebral metabolites. Combined HMO and lactoferrin supplementation was also associated with altered regional metabolite profiles, although their independent contributions remain uncertain. Structural MRI, diffusion tensor imaging, and myelin-sensitive imaging findings were heterogeneous, predominantly region-specific, and frequently nonsignificant. Potential mechanisms involving microbial metabolites, Sia availability, ganglioside metabolism, neural cell adhesion molecule polysialylation, neuroinflammation, and synaptic plasticity, remain hypothesis-generating rather than causally established. Conclusions: Current preclinical evidence suggests that HMO-containing interventions may influence selected neuroimaging outcomes but does not establish consistent improvements in neurodevelopment. Methodological heterogeneity limits cross-study comparisons and the absence of eligible human intervention studies limit clinical translation. Longitudinal investigations integrating neuroimaging, molecular profiling, and functional assessments are needed to clarify the imaging-based neurodevelopmental relevance of HMOs.

Check for updates

Academic Editor: Alice Monzani

Received: 21 October 2026
Revised: 11 November 2026
Accepted: 17 November 2026
Published: 20 November 2026

**Copyright:** © 2026 by the authors. Licensee MDPI, Basel, Switzerland. This article is an open access article distributed under the terms and conditions of the Creative Commons Attribution (CC BY) license.

**Keywords:** human milk oligosaccharides; magnetic resonance imaging (MRI); diffusion tensor imaging (DTI); magnetic resonance spectroscopy (MRS); preclinical model; neurodevelopment; neuroimaging

## 1. Introduction

Human milk oligosaccharides (HMOs) are the third most abundant solid component in breast milk, comprising over 200 structurally diverse glycans that are predominantly neutral fucosylated, neutral nonfucosylated, and sialylated types [1–3]. These complex carbohydrates represent one of the most significant compositional differences between human milk and infant formula, with concentrations ranging from ~20–25 g/L in colostrum to 5–20 g/L in mature milk, whereas cow's milk and cow's milk-based infant formulas contain oligosaccharides at levels 100–1000 times lower [4–6]. Although indigestible by the infant, HMOs act as selective substrates for gut microbiota, shaping microbial composition and driving the production of neuroactive metabolites, such as short-chain fatty acids (SCFAs) [7]. Interestingly, sialylated HMOs extend their functional influence independent of gut microbiota [8]. These molecules have been shown to enhance polysialylation of neural cell adhesion molecules (NCAMs), elevate brain ganglioside expression, and induce hippocampal microstructural changes indicative of enhanced neurodevelopment [9–12]. Such neurodevelopmental influence has been explored across macrostructural, microstructural, and molecular domains using an integrative toolkit of cognitive assessments, electrophysiological recordings, advanced neuroimaging modalities, and transcriptomic analyses.

Advanced neuroimaging modalities—including structural magnetic resonance imaging (MRI), diffusion tensor imaging (DTI), and magnetic resonance spectroscopy (MRS)—have become invaluable tools for characterizing neurodevelopment non-invasively with high spatial and functional resolution. T1-weighted MRI enables the detection of macrostructural changes, revealing volumetric alterations across distinct brain regions. In contrast, DTI leverages diffusion of water along axonal pathways to map white matter architecture, offering insights into fiber coherence and axonal maturation [13]. Complementing these structural techniques, MRS serves as a non-invasive window into the brain's metabolic landscape, quantifying neurochemicals such as *N*-acetylaspartate (NAA), glutamate (Glu), choline (Cho), and myo-inositol (mI)—metabolites tightly linked to neuronal viability, glial health, and synaptic function [14]. Together, these techniques have become indispensable in charting how the developing brain responds to early-life nutritional interventions, particularly HMOs, offering a window into their impact on neural architecture and metabolism.

Previous reviews have highlighted the potential neurodevelopmental relevance of HMOs but differ in scope and analytical focus. Fan et al. (2023) synthesized 26 preclinical and human observational studies examining the relationships between milk oligosaccharides and cognitive development, brain structure, and underlying biological mechanisms [15]. Subsequently, Xu et al. (2025) examined HMO structural diversity, compositional variation, and neurodevelopmental effects, with emphasis on gut–brain interactions and associated molecular pathways [16]. More recently, Suryawan et al. (2026) reviewed 18 preclinical and clinical studies covering cognitive, behavioral, neurobiological, and neuroimaging outcomes, including structural and microstructural brain development [17]. Despite these contributions, neuroimaging evidence has not been systematically appraised as a distinct outcome domain. In particular, the consistency and robustness of imaging findings, the influence of HMO composition and intervention design, and their relevance to proposed neurodevelopmental mechanisms remain unclear.

This review critically synthesizes neuroimaging evidence on the impact of individual and combined HMOs on neurodevelopment and cognitive functions in preterm and term infants and animal models. This review specifically focuses on structural MRI, DTI, myelin-sensitive imaging, and MRS to examine potential HMO-associated changes in brain structure and metabolism. We evaluate how differences in HMO composition and dose, developmental timing, imaging acquisition, and analytical approaches may contribute to inconsistent findings across studies. We distinguish directly observed neuroimaging outcomes from proposed biological mechanisms and identify key knowledge gaps and methodological priorities to improve translation from preclinical models to human infant studies. Finally, we delineate priorities for future research to elucidate the neurodevelopmental effects of HMOs.

## 2. Methods

### *2.1. Literature Search Strategy*

A systematic literature search was conducted in accordance with the Preferred Reporting Items for Systematic Reviews and Meta-Analyses (PRISMA 2020) guidelines to identify studies investigating the effects of HMOs on brain development using neuroimaging techniques. PubMed (National Library of Medicine), MEDLINE (Ovid), and Scopus (Elsevier) were searched from database inception to 1 November 2026.

Database-specific search strategies were developed using combinations of free-text terms and Boolean operators (AND/OR), with search fields adapted to the indexing and search functionalities of each database. Two principal concepts were targeted: (1) HMOs and their individual constituents, including 2′-fucosyllactose (2′-FL), 3′-sialyllactose (3′-SL), 6′-sialyllactose (6′-SL), lacto-*N*-tetraose (LNT), and lacto-*N*-neotetraose (LNnT), and (2) neuroimaging modalities and brain-related outcomes, including magnetic resonance imaging (MRI), diffusion tensor imaging (DTI), magnetic resonance spectroscopy (MRS), diffusion MRI, myelin water fraction, voxel-based morphometry, brain development, brain volumes, and brain metabolism.

Searches were performed primarily using title and abstract fields in PubMed ([tiab]), title, abstract, and keyword fields in Scopus (TITLE-ABS-KEY), and text-word fields in Ovid MEDLINE (.tw.). No controlled vocabulary headings were explicitly incorporated. No restrictions were applied by publication type, language, or population. Complete database-specific search strategies, including search terms, Boolean operators, search fields, search dates, platforms, and numbers of records retrieved, are provided in Supplementary Table S1.

Records retrieved from all three databases were imported into Covidence systematic review software (Veritas Health Innovation, Melbourne, Australia; https://www.covidence.org/) for duplicate identification and removal before title and abstract screening. Reference lists of included studies were not systematically screened, and no additional records were identified through citation searching. The study identification and selection process is presented in the PRISMA 2020 flow diagram (Figure 1).

### *2.2. Study Selection and Data Extraction*

Two reviewers independently screened titles and abstracts and subsequently assessed full texts articles against predefined PICOS eligibility criteria (Table 1). Eligible studies investigated HMO-containing interventions against appropriate comparators and reported brain-related outcomes assessed using neuroimaging techniques. Observational studies, reviews, and studies lacking eligible interventions, comparators, or neuroimaging outcomes were excluded. Disagreements were resolved by discussion and consensus, with consultation of a third reviewer when necessary.

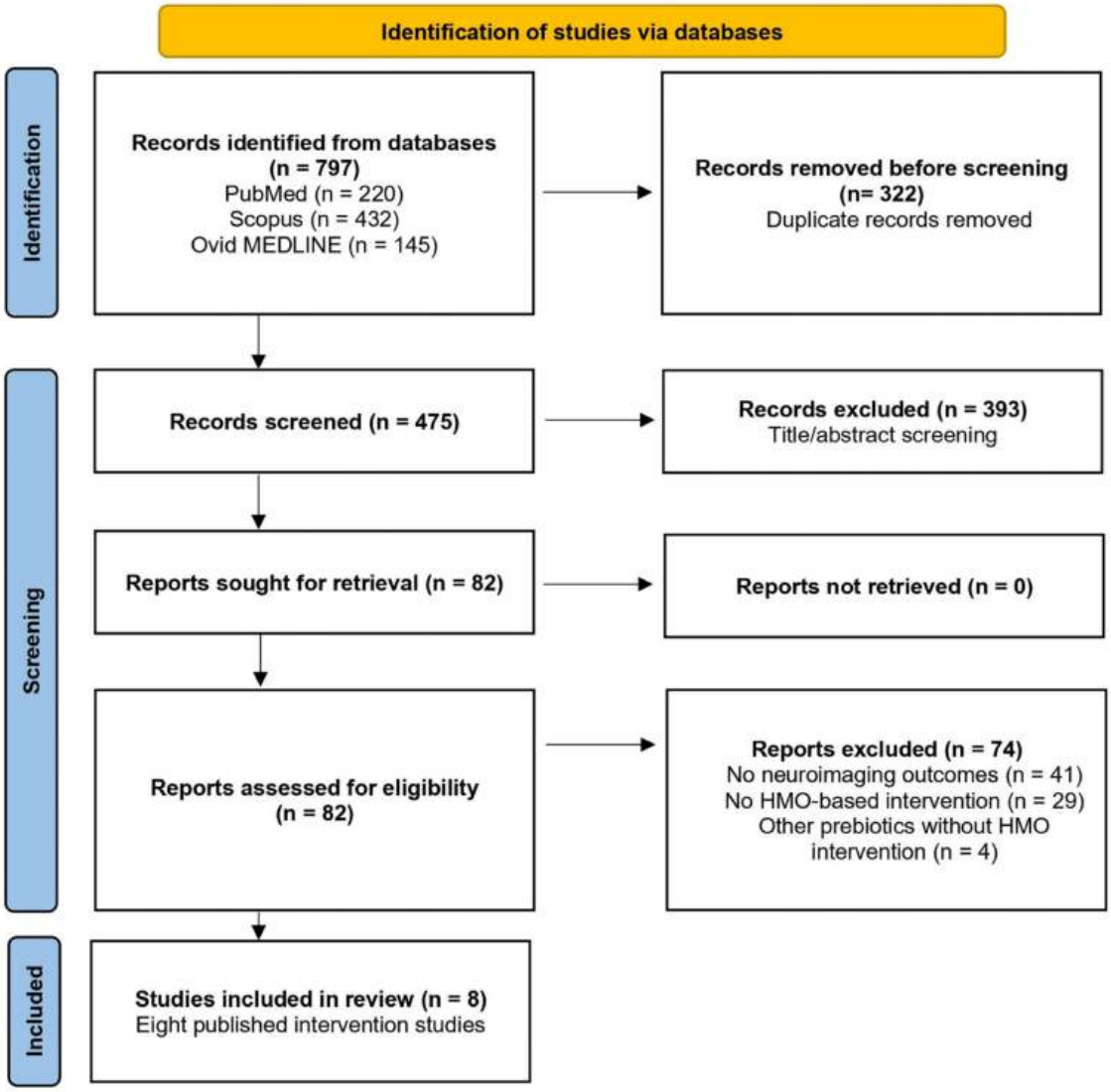



**Figure 1.** PRISMA (Preferred Reporting Items for Systematic Reviews and Meta-Analyses) flow chart.

**Table 1.** Summary of inclusion and exclusion criteria for studies included in the review.

| PICOS Element | Inclusions | Exclusions |
|---|---|---|
| Population | Infants, children, and healthy humans or animals (preterm or term). | Animals or humans with neurological, metabolic, or genetic disorders (e.g., Alzheimer's disease, autism spectrum disorder, diabetes, brain injury, infection, or any disease model). |
| Intervention | Studies including at least one intervention arm receiving individual or combined HMOs, either alone or with other nutritional or bioactive components. | Studies without an intervention arm containing human milk oligosaccharides (HMOs). |
| Comparator | Studies including at least one non-HMO comparator group, such as an unsupplemented control or a group receiving other nutritional or bioactive components without HMOs. | Studies lacking an appropriate non-HMO comparator group. |

**Table 1.** *Cont.*

| PICOS Element | Inclusions | Exclusions |
| --- | --- | --- |
| Outcome | Neurodevelopmental outcomes assessed via neuroimaging modalities (MRI, DTI, or MRS). | Neurodevelopmental outcomes assessed solely via cognitive testing, transcriptomics, or electrophysiology, without neuroimaging. |
| Study design | Human interventional studies and preclinical animal intervention studies. | Observational studies, reviews, conference abstracts, expert opinions, and letters to the editor. Observational evidence may be discussed for contextual purposes but is excluded from systematic synthesis. |

Data were independently extracted by two reviewers using a standardized extraction template. Extracted variables included study characteristics, experimental models or populations, intervention and comparator details, HMO composition and dosage, intervention duration, neuroimaging methods, brain regions assessed, and statistically significant and nonsignificant imaging outcomes. Extracted information was cross-checked against the original publications, and discrepancies were resolved by consensus.

### *2.3. Data Preparation and Synthesis*

A structured narrative synthesis was conducted across the eight included studies, with findings organized by neuroimaging modality (structural MRI, DTI, myelin-sensitive imaging, and MRS), brain region, and HMO intervention characteristics. Imaging outcomes were summarized according to the direction and magnitude of reported effects, statistical significance, and consistency across studies, considering differences in HMO composition, dosage, developmental timing, and imaging methodologies. Original measurement units and reported statistics were retained, and no data conversions or imputations were performed. Where numerical estimates were unavailable, findings were summarized qualitatively. Substantial heterogeneity in experimental designs, intervention characteristics, imaging protocols, and outcome measures precluded quantitative synthesis; therefore, no meta-analysis or standardized effect sizes were calculated. No formal sensitivity analyses were conducted because of the limited number of eligible studies and considerable methodological heterogeneity. Interpretation focused on consistency, biological relevance, and methodological quality of neuroimaging findings, rather than statistical significance alone.

### *2.4. Risk-of-Bias Assessment*

Risk of bias in the eight included studies was independently assessed by two re-viewers using SYRCLE's risk-of-bias tool, which evaluates ten domains covering selection, performance, detection, attrition, reporting, and other potential sources of bias. Assessments were based on information reported in the original publications. Discrepancies were resolved through discussion and consensus. Each domain was classified as having low, high, or unclear risk of bias, with study-specific assessments presented in Supplementary Table S2.

### *2.5. Review Registration and Protocol*

The review was not registered, and no formal protocol was prepared.

## 3. Results

### *3.1. Study Selection*

The database searches identified 797 records (PubMed: 220; Scopus: 432; Ovid MEDLINE: 145). After removing 322 duplicates, 475 unique records were screened, of which 82

articles were selected for full-text assessment. Following full-text review, 74 articles were excluded for the following reasons: absence of neuroimaging outcomes (n = 41), no HMO intervention (n = 29), or investigation of prebiotics other than HMOs (n = 4). Consequently, eight studies met the eligibility criteria and were included in the final review. An overview of the included studies is presented in Figure 2, while their detailed characteristics and neuroimaging findings are summarized in Table 2.

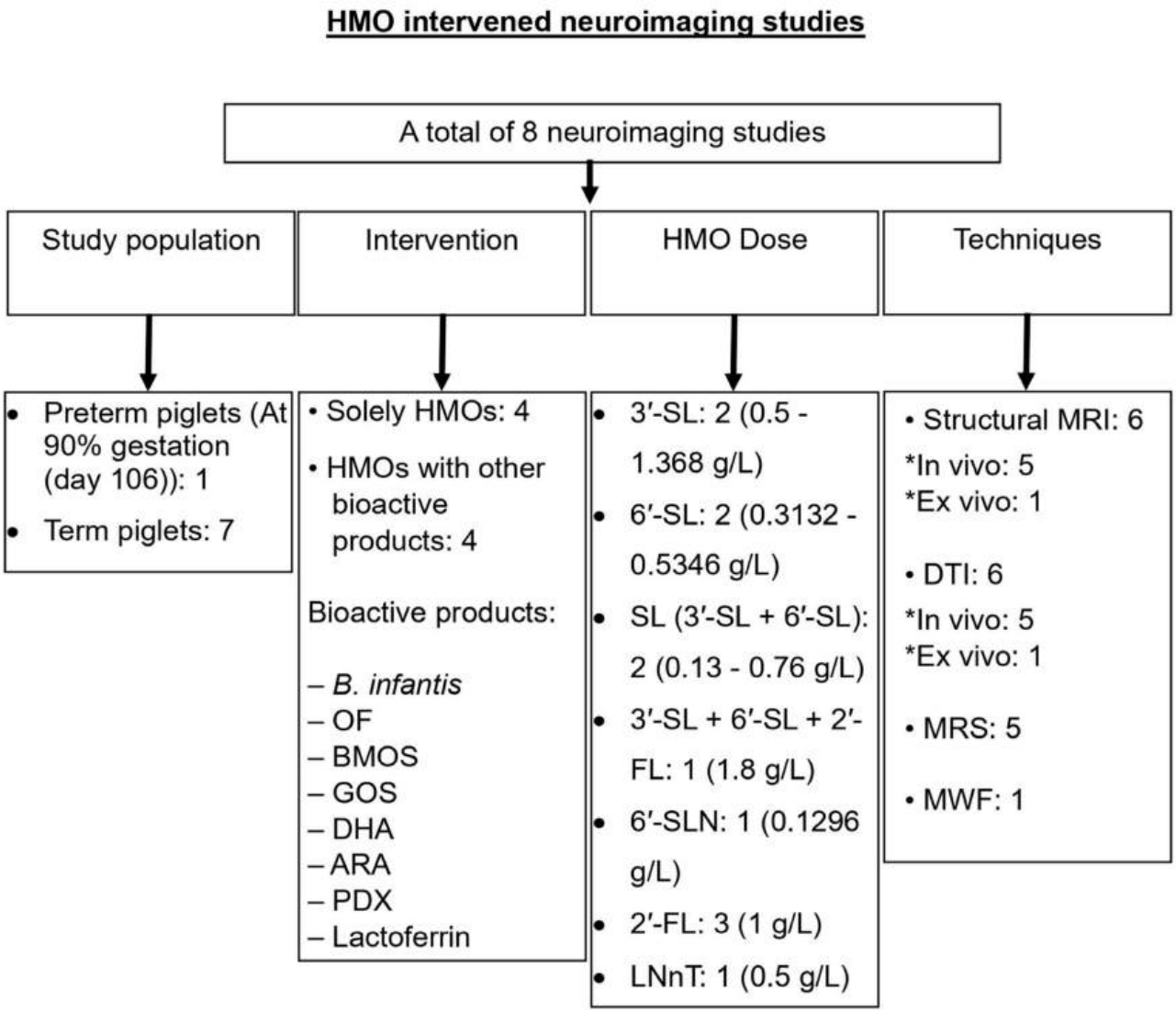



**Figure 2.** Summary of the number of HMO intervention neuroimaging studies focusing on study population, intervention types, HMO dosage (dose ranges in parentheses), and neuroimaging techniques. HMOs = human milk oligosaccharides; *B. infantis* = *Bifidobacterium infantis*; OF = oligofructose; BMOS = bovine milk oligosaccharides; GOS = galactooligosaccharide; DHA = docosahexaenoic acid; ARA = arachidonic acid; PDX = polydextrose; 3′-SL = 3′-sialyllactose; 6′-SL = 6′-sialyllactose; SL = sialyllactose; 6′-SLN = 6′-sialyllactosamine; 2′-FL = 2′-fucosyllactose; LNnT = lacto-N-neotetraose; MRI = magnetic resonance imaging; DTI = diffusion tensor imaging; MRS = magnetic resonance spectroscopy; MWF = myelin water fraction. *: For each modality, imaging studies were subdivided into in vivo (n = 5) and ex vivo (n = 1).

**Table 2.** Characteristics of HMO intervention studies in preclinical animal models using neuroimaging techniques.

| Author, Year, and Country | Study Design (Sample Size, No. of ROI and Age at MRI) | Intervention and Parameters | Main Outcomes | Principal Nonsignificant Findings |
| --- | --- | --- | --- | --- |
| 1. Amin et al. (2026) [18]; Australia | 44 male piglets; Age at MRI: PND 38/39 | Ctrl (methylcellulose, 1.8 g/L), combined HMOs (70% 2′-FL and 30% 3′-SL:6′-SL in a 1:2.5 ratio, 1.8 g/L), combined HMOs (1.8 g/L) + lactoferrin (0.5 g/L); MRS | cHMOs + Lf vs. control: Higher absolute tLM and relative tCr, tCho, and tLM concentration ($p < 0.05$; post hoc comparison).<br>cHMOs + Lf vs. cHMOs: Higher relative GSH, tCr, and tLM concentration ($p < 0.05$; post hoc comparison).<br>cHMOs vs. cHMOs + Lf: Higher absolute tNAA concentration ($p < 0.05$; post hoc comparison) | Numerically higher concentration: Ala, Cr, Lip, and MM (cHMOs + Lf vs. control and cHMOs); GABA, NAAG, SI, and Tau (cHMOs vs. control and cHMOs + Lf); Glu, Gln, and Glx (Control vs. cHMOs and cHMOs + Lf). |
| 2. Golden et al. (2023) [19]; USA | 75 male piglets; 26 ROI; Age at MRI: PND 30 and 58 | Ctrl, 3′-SL (PND 2–33: 500 mg/L; PND 33–61: 2.673 g/kg), 6′-SL (PND 2–33: 500 mg/L; PND 33–61: 2.673 g/kg); Structural MRI, DTI, MWF | 3′-SL → ↑ relative pons volume (PND 30); 6′-SL → ↑ relative cerebral aqueduct and midbrain volumes (PND 58)<br>PND 30: 6′-SL → ↓ FA (cerebellum, internal capsule, overall WM), 3′-SL → ↓ FA (internal capsule, overall WM);<br>PND 58: 3′-SL → ↓ FA (right hippocampus); 6′-SL → ↓ FA (right hippocampus, thalamus)<br>PND 58: 6′-SL → ↓ AD and MD in the cerebellum; ↓ AD, RD, and MD in the left hippocampus<br>PND 30: 3′-SL and 6′-SL → ↑ myelin content (left hippocampus, left superior colliculus) | No significant differences in myelin water fraction across brain regions at PND 58. Regional DTI measures (AD, MD, and RD) showed no significant dietary effects at PND 30. |

**Table 2.** *Cont.*

| Author, Year, and Country | Study Design (Sample Size, No. of ROI and Age at MRI) | Intervention and Parameters | Main Outcomes | Principal Nonsignificant Findings |
|---|---|---|---|---|
| 3. Sutkus et al. (2022) [20]; USA | 52 male piglets; 27 ROI; Age at MRI: PND 32 or 33 | Ctrl (Lactose 0.532%), 2′-FL (2′-FL, 1.0 g/L), BI: (*B. infantis* (Bi-26), $10^9$ CFU/pig/d), FLBI: (2′-FL, 1.0 g/L + Bi-26, $10^9$ CFU/pig/d); Structural MRI, DTI | 2′-FL → ↑ relative pons volume<br>Bi-26 → ↓ absolute volumes (corpus callosum, left caudate, left cortex, lateral ventricles, medulla, internal capsules, putamen-globus pallidus) and relative volume (putamen-globus pallidus) | No significant differences in whole-brain, GM, WM, or CSF volumes.<br>No significant 2′-FL × Bi-26 interaction for regional brain volumes. |
| 4. Fleming et al. (2020) [21]; USA | 36 male piglets; 22 ROI; Age at MRI: PND 32 or 33 | Ctrl, OF (5 g/L), OF + 2′-FL (OF, 5 g/L + 2′-FL, 1 g/L); Structural MRI, DTI, MRS | OF and OF + 2′-FL vs. control → ↑ relative olfactory bulbs volumes | No effect of diet for any DTI measure.<br>No significant differences in MRS-derived metabolites concentration. |
| 5. Fleming et al. (2020) [22]; USA | 48 male piglets; 23 ROI; Age at MRI: PND 32 or 33 | Ctrl, BMOS (12.4 g/L), HMO (2′-FL, 1.0 g/L + LNnT, 0.5 g/L), BMOS + HMO (BMOS, 12.4 g/L + 2′-FL, 1.0 g/L + LNnT, 0.5 g/L); Structural MRI, DTI, MRS | BMOS and BMOS + HMO → ↓ absolute lateral ventricle volumes | No significant dietary effects on DTI-derived indices of brain microstructure or MRS-derived brain metabolite concentrations. |
| 6. Wang et al. (2019) [23]; Australia | 46 male piglets; Age at MRI: PND 38/39 | Ctrl, SL (3′-SL, 7.6 g/kg + 6′-SL, 1.9 g/kg), SL/SLN (3′-SL, 7.04 g/kg + 6′-SL, 1.74 g/kg + 6′-SLN, 0.72 g/kg); MRS | SL and SL/SLN → ↑ absolute and relative concentration (mIns, Glu, and Glx)<br>Total white matter volume ∝ NAA, total NAA, mIns, total Cho, total Cr, SI, and Glth; whole-brain volume ∝ Glu and SI; whole-brain weight ∝ SI | Absolute concentration of tNAA, PCr, SI, and tCho was 3–6%, 3–15%, 3–9%, and 2–7% higher in the treatment groups compared with the control group. |

**Table 2.** *Cont.*

| Author, Year, and Country | Study Design (Sample Size, No. of ROI and Age at MRI) | Intervention and Parameters | Main Outcomes | Principal Nonsignificant Findings |
|---|---|---|---|---|
| 7. Obelitz-Ryom et al. (2019) [10]; Denmark | 66 piglets (male and female);<br>Age at MRI: After PND 19 | PRE-CON (Raw bovine milk + 6 g/L lactose),<br>PRE-SAL (Raw bovine milk + 8.5 g/L oligosaccharide-enriched whey (380 mg SL/L)),<br>TERM-CON (Raw bovine milk + 6 g/L lactose),<br>TERM-NAT (Naturally breastfed);<br>Ex vivo (right cerebral hemisphere) MRI and DTI | TERM-NAT vs. TERM-CON → ↑ hippocampus and prefrontal cortex volume | No significant differences in MRI-derived regional brain volumes or diffusion-derived measures between PRE-SAL and PRE-CON groups. |
| 8. Mudd et al. (2017) [24]; USA | 38 male piglets;<br>19 ROI;<br>Age at MRI: PND 32 or 33 | Ctrl (DHA, 174 mg/L; ARA, 348 mg/L; GOS, 2 g/L; PDX, 2 g/L),<br>LOW (Control diet + 130 mg/L SL),<br>MOD (Ctrl diet + 380 mg/L SL),<br>HIGH (Ctrl diet + 760 mg/L SL)<br>(* SL = Bovine-derived modified whey enriched with SL);<br>Structural MRI, VBM, MRS, DTI, TBSS | MOD SL vs. control, LOW SL and High SL→ ↑ AD and MD (corpus callosum)<br>MOD SL vs. control and LOW SL → ↑ RD (corpus callosum)<br>In VBM, LOW SL vs. MOD SL → ↑ gray matter (right cortex and midbrain), ↑ white matter (caudate and midbrain); MOD SL vs. LOW SL → ↑ gray matter (left cortex), ↑ white matter (pons)<br>In TBSS, MOD SL vs. LOW SL → ↑ RD (left hemisphere corpus callosum) | No significant differences in MRS-assessed brain metabolite profiles.<br>No significant differences in absolute or relative whole-brain or regional brain volumes.<br>No significant differences in DTI-derived FA across assessed brain regions.<br>A trend ($p = 0.06$) toward increased relative left cortical volume in piglets supplemented with SL. |

US = United States; CFU = colony-forming unit; DTI = diffusion tensor imaging; MWF = myelin water fraction; FA = fractional anisotropy; MD = mean diffusivity; AD = axial diffusivity; RD = radial diffusivity; VBM = voxel-based morphometry; TBSS = tract-based spatial statistics; MRI = magnetic resonance imaging; MRS = magnetic resonance spectroscopy; 3′-SL = 3′-sialyllactose; 6′-SL = 6′-sialyllactose; 2′-FL = 2′-fucosyllactose; 6′-SLN = 6′-sialyllactosamine; LNnT = lacto-N-neotetraose; OF = oligofructose; BMOS = bovine milk oligosaccharides; HMO = human milk oligosaccharides; *B. infantis* = *Bifidobacterium infantis*; ROI = region of interest; mIns = myo-inositol; Glx = glutamate + glutamine; NAA = N-acetylaspartate; Cho = choline; Cr = creatine; SI = scyllo-inositol; Glu = glutamate; DHA = docosahexaenoic acid; ARA = arachidonic acid; GOS = galactooligosaccharide; PDX = polydextrose; ∝ = positive correlation; WM = white matter; Lf = lactoferrin. *: In Mudd et al. (2017) [24], SL was administered as SL-enriched bovine modified whey, not in purified form.

### *3.2. Risk-of-Bias in the Included Studies*

All eight studies were rated as having a low risk of bias for baseline characteristics and investigator blinding, and seven were rated as low risk for outcome-assessor blinding. Random sequence generation, incomplete outcome data, and other potential sources of bias were consistently rated as unclear. Allocation concealment, random housing, and random outcome assessment were rated as unclear in five, six, and five studies, respectively. Selective reporting was rated as low risk in seven studies. No high-risk judgments were recorded. However, the frequent unclear ratings indicate limitations in methodological reporting (Supplementary Table S2).

### *3.3. Methodological Limitations and Quality of Evidence*

Despite strengths in baseline comparability and blinding, incomplete reporting of randomization, allocation concealment, outcome assessment, and attrition limits confidence in the methodological quality of the included studies. Although selective reporting was evaluated at the study level using SYRCLE, reporting bias across the evidence synthesis and overall certainty of evidence was not formally assessed. The small number of studies, heterogeneity in neuroimaging outcomes, and absence of eligible human intervention studies further constrain interpretation and generalizability of the findings. Future investigations should prioritize transparent methodological reporting, harmonized neuroimaging protocols, and adequately powered longitudinal studies to strengthen reproducibility and clinical translation.

### *3.4. Methodological Difference of HMO Intervened Neuroimaging Studies*

Eight neuroimaging studies have examined the effect of HMO interventions on brain outcomes in neonatal piglets. Four of these studies investigated sialylated HMOs—specifically 3′-SL, 6′-SL, and 6′-sialyllactosamine (6′-SLN) [10,19,23,24]—whereas three focused primarily on fucosylated HMOs, particularly 2′-FL, administered alone or with LNnT [19,23,24]. More recently, Amin et al. (2026) investigated a combined HMOs (cHMOs) formulation containing 70% fucosylated and 30% sialylated HMOs [18].

Sialylated HMO supplementation strategies varied considerably across studies, including single-component 3′-SL or 6′-SL [19], dual administration of 3′-SL and 6′-SL [10,24], a complex blend of 3′-SL, 6′-SL, and 6′-SLN [23], and the combined administration of 3′-SL, 6′-SL, and 2′-FL [18]. Ratios of 3′-SL to 6′-SL also differed, including 4:1 [23] or 6:1 [10] or 1:2.5 [18], and doses range from 130 mg/L to 1710 mg/L, depending on formulation and study protocol [10,18,19,23,24]. Among studies focusing on fucosylated HMOs, 2′-FL was generally administered at 1 g/L, with LNnT provided at 0.5 g/L when included [20–22]. In the fucosylated and sialylated combined study, 1.26 g/L 2′-FL was administered [18]. HMO-supplemented diets were compared with a range of controls, including standard commercial milk replacers [19,21–23], commercial formulas with 0.532% lactose [20], commercial formulas with methyl cellulose [18], formulations enriched with docosahexaenoic acid (DHA), arachidonic acid (ARA), galactooligosaccharide (GOS), and polydextrose (PDX) [24], or raw bovine milk supplemented with 6 g/L lactose [10].

All studies employed in vivo MRI in term male piglets, except Obelitz-Ryom et al. (2019), who conducted ex vivo imaging, restricted to the right cerebral hemisphere, on both sexes of preterm piglets [10]. MRI scans were most commonly performed around postnatal day (PND) 32–33, although timing varied slightly across studies. Amin et al. (2026) and Wang et al. (2019) conducted $^{1}$H-MRS at PND 38/39, Obelitz-Ryom et al. (2019) initiated ex vivo scans after PND 19, and Golden et al. (2023) implemented a longitudinal design with scans at both PND 30 and 58 [10,18,19,23]. Field strengths ranged from 3T MRI for in vivo scans to 9.4T for ex vivo imaging and anesthesia protocols varied from

intramuscular telazol (with or without ketamine and xylazine for induction) [19–22,24] to inhaled isoflurane maintenance at 2–3.5% [18,23]. Structural imaging used T1-weighted in vivo MPRAGE (magnetization-prepared rapid gradient-echo) sequences with TR (repetition time) 1900–2060 ms, TE (echo time) 2.05–6.5 ms, and isotropic voxel sizes of 0.6–0.7 mm [19–22,24]. Ex vivo sequences achieved higher resolution (0.26 mm voxel) with shorter TR/TE (3.6 ms/1.8 ms) [10]. Brains were segmented into 19–27 regions of interest (ROIs) using the pig brain atlas [19–22,24]. Diffusion-weighted imaging commonly employed b-values of 1000 and 2000 s/mm$^2$ with 30 directions (voxel size = 1.6–2 mm), while ex vivo imaging applied up to 12 b-values (up to 15,000 s/mm$^2$) and 8 directions per level for high-resolution tract mapping [10].

For spectroscopy, three studies (Fleming et al. (2020) and Mudd et al. (2017)) used a spin-echo chemical shift sequence centered over the dorsal hippocampus (voxel: 20 mm × 23 mm × 13 mm), with TR/TE values of 1800 ms/68 ms for water-suppressed scans and 20,000 ms/68 ms for non-suppressed [21,22,24]. In contrast, Amin et al. (2026) and Wang et al. (2019) applied point-resolved spectroscopy (PRESS) sequence (TR = 2000 ms; voxel: 15 mm × 14 mm × 20 mm) targeting frontal lobe gray and white matter; however, the studies differed substantially in echo time (TE) [18,23]. Wang et al. (2019) employed a long-TE acquisition of 270 ms, whereas Amin et al. (2026) used a short-TE acquisition of 30 ms [18,23]. Spectral analyses were performed using LCModel with Cramer–Rao lower bounds (CRLB) < 20% defining reliable quantification [21,22,24] or TARQUIN (without CRLB) for automated long and short echo-time fitting [18,23]. Advanced imaging techniques included myelin water fraction (MWF) mapping derived from multi-angle spoiled gradient-recalled echo (SPGR) and steady-state free precession (SSFP) sequences, providing a novel MRI-based measure of myelin content following SL supplementation [19]. To characterize structural brain alterations at high spatial resolution, Mudd et al. (2017) employed voxel-based morphometry (VBM) to quantify gray and white matter tissue concentrations, together with tract-based spatial statistics (TBSS) to identify microstructural diffusion differences between treatment groups [24]. The anesthesia protocols and neuroimaging acquisition parameters employed across the eight included studies are summarized in Table 3.

Collectively, this substantial heterogeneity in acquisition protocols, anatomical targets, echo times, spectral quantification methods, and image-processing approaches limits cross-study comparability and complicates the attribution of observed neuroimaging differences specifically to HMO exposure. Accordingly, the observed findings should be interpreted cautiously as preliminary and hypothesis-generating unless replicated using harmonized experimental and neuroimaging protocols.

### *3.5. Structural MRI Reveals Region-Specific Sensitivity to HMO Supplementation*

In neonatal pig models, multimodal neuroimaging has revealed region-specific neurodevelopmental responses to HMO supplementation. T1-weighted MRI has been widely employed to investigate the effects of varying doses of sialylated and fucosylated HMOs on both absolute and relative brain volumes across cortical and subcortical regions. Despite the sensitivity of T1-weighted images to early macrostructural changes [13], dietary SL supplementation exerted minimal effects on global brain volumetric development in both term and preterm piglets [10,19,24]. Significant changes were observed only in a limited number of regions—including the pons, cerebral aqueduct, and midbrain—which exhibited increased relative volumes following SL supplementation ($p < 0.05$) [19]. Several factors may explain these modest volumetric effects, including limited endogenous exposure to sialylated oligosaccharides in pigs, which may constrain the magnitude of HMO-induced macrostructural changes. Porcine milk naturally contains low levels of 3′-SL

(50–100 mg/L) and negligible amounts of 6′-SL [25], and the concentration of Sia in pig brains is nearly four times lower than that in human brains [26]. It is, therefore, conceivable that the SL doses supplemented in these studies (130–780 mg/L) were sufficient to meet baseline neurodevelopmental requirements in piglets, thereby limiting detectable differences between supplemented and control groups. Moreover, the majority of neurons are generated prenatally, and postnatal brain growth throughout the brain predominantly involves synaptogenesis, dendritic remodeling, and myelination rather than neurogenesis [27,28]. Consequently, postnatal SL supplementation may not substantially influence neurogenesis-linked endpoints, such as global and region-specific brain volumes. Another important consideration when interpreting HMO-associated neuroimaging outcomes is the composition of the background experimental diets. In Mudd et al. (2017), both control and SL-supplemented diets contained DHA, ARA, GOS, and PDX, all of which may influence neurodevelopment through effects on neuronal membrane maturation, cellular signaling, and microbiota–gut–brain interactions [24,29,30]. As these ingredients were provided at comparable concentrations across experimental groups, they are unlikely to explain between-group differences independently. However, potential interactions with SL may have modified the neurodevelopmental response. Whether these dietary components influenced the magnitude or statistical significance of the observed neuroimaging outcomes remains unknown [24].

Similar to sialylated HMOs, fucosylated HMOs induce modest yet region-specific volumetric changes in the developing brain. Notably, 2′-FL supplementations have been linked to increased relative volumes of the olfactory bulbs and pons [20,21]. These findings suggest that brain regions undergoing rapid postnatal maturation may be selectively responsive to HMO exposure during critical developmental windows, while other regions may require prolonged exposure to manifest detectable structural or functional changes [31]. Accordingly, extending the duration of supplementation may be necessary to reveal HMO-related structural or functional effects in slower-maturing brain regions [31]. Besides, a main effect of HMO supplementation was reflected in increased relative volumes of the corpus callosum and cortical regions, suggesting a consistent influence on brain structures undergoing rapid postnatal growth. In contrast, significant interaction effects between HMOs and bovine milk oligosaccharides (BMOs) were observed for the absolute volumes of subcortical structures—including the caudate, hypothalamus, thalamus, and total gray matter—indicating that the co-administration of distinct prebiotics may synergistically modulate neurodevelopment beyond their individual effects.

Furthermore, the addition of *Bifidobacterium infantis* (Bi-26), or BMOs, was associated with reductions in both absolute and relative volumes of several brain regions. Although the underlying mechanisms remain poorly understood, the associations may reflect altered gut–brain signaling or complex interactions with co-administered HMOs. A major confounding factor across these studies is the inconsistency in total oligosaccharide dosage among treatment groups, with piglets receiving markedly different total doses for each source of oligosaccharides, including HMOs (1.5 g/L), BMOs (12.4 g/L), BMOs + HMOs (13.9 g/L), oligofructose (OF, 5 g/L), and OF + HMOs (6 g/L). Consequently, observed differences in neuroanatomical outcomes may be driven by total oligosaccharide load rather than the specific oligosaccharide composition, which highlights the importance of dose-controlled study designs in future investigations aimed at optimizing dietary interventions in early-life brain development. Moreover, suboptimal dosing of 2′-FL and the use of different control diets further confound cross-study comparisons [20–22] and may partially explain the lack of robust volumetric responses following fucosylated HMO intervention. In general, volumetric MRI may lack sufficient sensitivity to detect early HMO-related short-term effects, which may instead manifest at the microstructural level (e.g., synaptic

organization and myelination) or molecular level (e.g., gene expression and neurotransmitter metabolism)—before macroscopic changes are detectable by conventional T1-weighted imaging. Brain regions showing sensitivity to HMO supplementation are summarized in Figure 3.

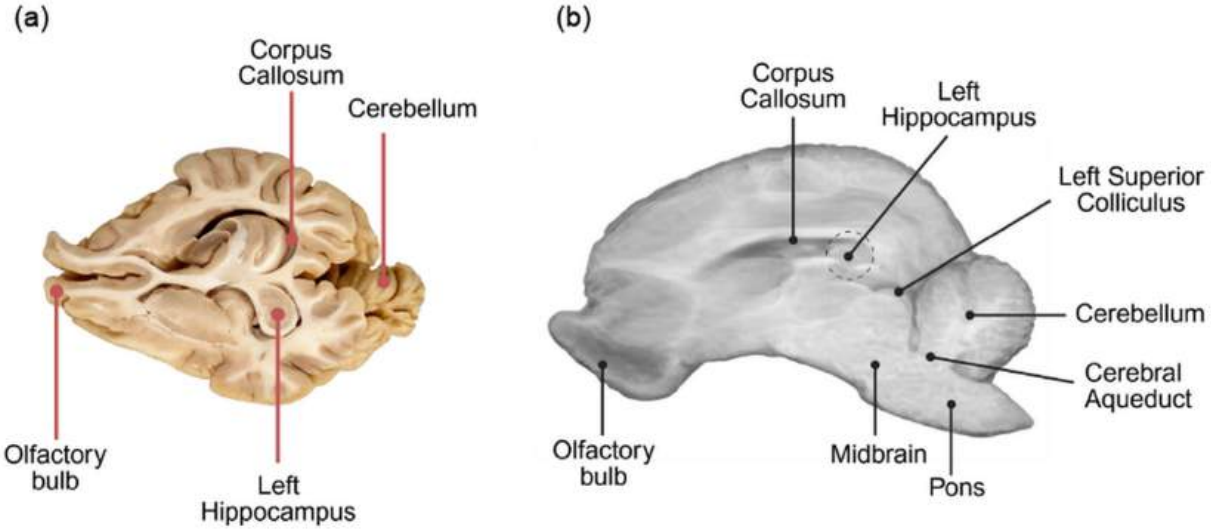



**Figure 3.** Schematic diagram of the piglet brain showing subregions sensitive to dietary HMO exposure. (**a**) Schematic representation of the brain subregions in the axial plane. (**b**) Corresponding brain regions visualized primarily using T1-weighted imaging in the sagittal plane. The dotted outline indicates the approximate location of the hippocampus.

Voxel-based morphometry (VBM) is an automated, whole-brain MRI analysis technique that quantifies regional differences in gray and white matter volume by statistically comparing tissue composition on a voxel-wise basis. Using this approach, Mudd et al. (2017) [24] revealed distinct, region-specific differences in gray and white matter concentrations between piglets receiving low- and moderate-dose SL diets. Notably, piglets receiving a lower dose of SL exhibited more extensive and larger gray matter clusters in the right cortex and midbrain compared to those receiving the moderate-dose diet [24]. Because axonal growth and synaptic pruning dynamically shape gray matter composition during neurodevelopment [24], future studies should incorporate molecular markers of these processes to determine whether the reduced tissue concentrations observed in piglets receiving moderate-dose SL reflect pruning-related elimination or attenuated axonal expansion.

Overall, structural MRI evidence suggests potential region-specific associations with HMO supplementation, but no consistent effect on global brain volume has been demonstrated. Reported regional differences are largely study-specific and lack independent replication. Heterogeneity in HMO composition and dosage, control diets, and developmental timing further constrain cross-study comparability. Accordingly, current evidence remains insufficient to establish a reproducible HMO-associated brain macrostructural phenotype.

**Table 3.** Anesthesia protocols and imaging sequences used in HMO intervention studies in preclinical animal models employing neuroimaging techniques.

| Author, Year | Induction and Maintenance of Anesthesia | 3D T1-Weighted MPRAGE Sequence | DWI-EPI Sequence | Other Sequences |
|---|---|---|---|---|
| 1. Amin et al. (2026) [18] | Induction: 5% isoflurane (inhalation), maintenance: 2–3.5% isoflurane (inhalation) | - | - | MRS single-voxel spin echo PRESS sequence: TR 2000 ms, TE 30 ms, voxel volume (15 mm × 14 mm × 20 mm), centered over the frontal lobe gray and white matter |
| 2. Golden et al. (2023) [19] | Induction: Telazol:ketamine:xylazine solution (IM, 0.03 mL/kg BW); maintenance: 2% isoflurane (inhalation) | TR = 2060 ms, TE for PND30/PND58 = 2.05 ms/ 2.52 ms, 0.6 mm isotropic voxel | TE for PND30/PND58 = 78.20 ms/ 70 ms, TR for PND30/PND58 = 6180 ms/ 5100 ms, b = 1000 and 2000 s/mm$^2$ across 30 directions and 1 image with a b = 0 s/mm$^2$, 1.6 mm isotropic voxel | SSFP sequence: TR/TE = 5.3 ms/2.65 ms, α = 11–70°, voxel volume = 1.25 × 1.25 × 1.3 mm$^3$; SPGR sequence: TR/TE = 5.6 ms/2.7 ms, α = 3–18°, voxel volume = 1.25 × 1.25 × 1.3 mm$^3$; T1-weighted IR SPGR sequence: TR/TE/TI = 5.6 ms/2.7 ms/(450, 750) ms, α = 5°, voxel volume = 1.7 × 1.7 × 2.6 mm$^3$ |
| 3. Sutkus et al. (2022) [20] | Induction: Telazol:ketamine:xylazine solution (IM, 0.03 mL/kg BW); maintenance: 2% isoflurane (inhalation) | TR = 2000 ms, TE = 6.5 ms, 0.6 mm isotropic voxel | TR = 5100 ms, TE = 70 ms, b = 1000 and 2000 s/mm$^2$ across 30 directions, 1.6 mm isotropic voxel | - |
| 4. Fleming et al. (2020) [21] | Induction: Telazol (IM, 0.07 mL/kg BW); maintenance: 2% isoflurane (inhalation) | TR = 1900 ms, TE = 2.49 ms, 0.7 mm isotropic voxel | b = 1000 s/mm$^2$ across 30 directions, 2 mm isotropic voxel | MRS spin-echo chemical shift sequence: TR for WS/non-WS scan = 1800 ms/20,000 ms, TE = 68 ms, voxel volume (20 mm × 23 mm × 13 mm), centered over the left and right dorsal hippocampi |
| 5. Fleming et al. (2020) [22] | Induction: Telazol (IM, 0.07 mL/kg BW); maintenance: 2% isoflurane (inhalation) | TR = 1900 ms, TE = 2.49 ms, 0.7 mm isotropic voxel | b = 1000 s/mm$^2$ across 30 directions, 2 mm isotropic voxel | MRS spin-echo chemical shift sequence: TR for WS/non-WS scan = 1800 ms/20,000 ms, TE = 68 ms, voxel volume (20 mm × 23 mm × 13 mm), centered over the left and right dorsal hippocampi |

**Table 3.** *Cont.*

| Author, Year | Induction and Maintenance of Anesthesia | 3D T1-Weighted MPRAGE Sequence | DWI-EPI Sequence | Other Sequences |
|---|---|---|---|---|
| 6. Wang et al. (2019) [23] | Induction: 5% isoflurane (inhalation), maintenance: 2–3.5% isoflurane (inhalation) | - | - | MRS single-voxel spin echo PRESS sequence: TR 2000 ms, TE 270 ms, voxel volume (15 mm × 14 mm × 20 mm), centered over the frontal lobe gray and white matter |
| 7. Obelitz-Ryom et al. (2019) [10] | - | Spoiled 3D gradient echo sequence: TR/TE = 3.6 ms/1.8 ms, 0.26 mm isotropic voxel | 2D spin-echo sequence: 12 b-values up to 15,000 s/mm$^2$ and 8 directions per b-value, TR/TE = 7.5 s/55 ms, diffusion time = 40 ms, 0.625 mm isotropic voxel | - |
| 8. Mudd et al. (2017) [24] | Induction: Telazol (IM, 0.07 mL/kg BW); maintenance: 2% isoflurane (inhalation) | TR = 1900 ms, TE = 2.49 ms, 0.7 mm isotropic voxel | b = 1000 s/mm$^2$ across 30 directions, 2 mm isotropic voxel | MRS spin-echo chemical shift sequence: TR for WS/non-WS scan = 1800 ms/20,000 ms, TE = 68 ms, voxel volume (20 mm × 23 mm × 13 mm), centered over the left and right dorsal hippocampi |

BW = body weight; IR = inversion recovery; IM = intramuscular injection; MPRAGE = magnetization-prepared rapid gradient-echo; ms = millisecond; b-value = diffusion weightings; DWI-EPI = diffusion-weighted echo planar imaging; TR = repetition time; TE = echo time; TI = inversion time; α = flip angle; SSFP = steady-state free precession; SPGR = spoiled gradient-recalled echo; MRS = magnetic resonance spectroscopy; PRESS = point-resolved spectroscopy; WS = water-suppressed.

### *3.6. Microstructural Sensitivity of the Developing Brain to HMOs*

Diffusion tensor imaging (DTI) has emerged as a powerful modality to characterize the maturation of white matter architecture by quantifying the directionality of water diffusion along axonal tracts. Key DTI metrics—including axial diffusivity (AD), radial diffusivity (RD), mean diffusivity (MD), and fractional anisotropy (FA)—serve as proxies for microstructural features, such as axonal organization, fiber coherence, and myelination [32]. MD reflects the overall magnitude of water diffusion and typically declines as neural tissue density increases during development [33]. RD captures water diffusion perpendicular to axon bundles and decreases with progressive myelination, while AD, representing diffusion along the primary fiber axis, is influenced by axonal growth and organization during neurodevelopment [33]. FA, a composite index of diffusion directionality, increases with brain maturation and reflects increasing microstructural coherence within white matter tracts [33,34]. Importantly, DTI-derived metrics are sensitive but non-specific indices of tissue microstructure. FA, MD, AD, and RD are influenced by multiple factors, including fiber orientation and crossing, axonal packing, membrane density, extracellular water content, tissue geometry, and myelination. Therefore, changes in individual DTI metrics cannot independently establish specific alterations in myelination, axonal integrity, or developmental maturity without corroborating evidence from complementary imaging, histological, or molecular validation.

Piglet models receiving long-term HMO supplementation have demonstrated region-specific enhancements in white matter microstructure. For example, 6′-SL supplementation reduced MD and RD in the cerebellum at PND 58, findings that may be consistent with developmental changes in tissue microstructure, including myelin-related processes. Given the posterior-to-anterior trajectory of brain maturation, early microstructural sensitivity in the cerebellum is particularly noteworthy [31]. Similarly, diet-induced differences in diffusion metrics were observed for the left hippocampus, where piglets receiving 6′-SL exhibited lower MD, RD, and AD values compared with the control animals, whereas such effects were not observed for piglet's receiving 3′-SL supplementations. This finding aligns with the pronounced hippocampal growth observed in male pigs at approximately eight weeks of age [35], suggesting that HMO-related effects may be most detectable during periods of rapid regional maturation. As neurodevelopment progresses, the accumulation of cellular components and myelinated fibers increasingly restricts water diffusion, contributing to the expected developmental declines in MD and RD across maturing white matter regions [33]. In parallel, axonal growth and maturation are often accompanied by gradual decreases in axial diffusivity during brain development, reflecting increased axonal packing, greater cytoskeletal complexity, and reduced tissue water content rather than axonal injury [36].

On the contrary, DTI metrics appear largely unaffected by short term (four weeks) HMO intervention in most pig studies. Although Golden et al. (2023) reported reduced FA values in white matter regions, such as the cerebellum and internal capsule, following SL supplementation, these findings may reflect methodological factors, including image acquisition limitations, small sample size, or partial volume effects, associated with the relatively small size of these brain regions [19]. Similarly, Mudd et al. (2017) found no significant differences in diffusion values with higher or lower levels of SL treatment [24]. Although a moderate dose of SL (380 mg/L) displayed diffusion differences in corpus callosum, the observed values across different groups appear to be within the normative developmental range. These diffusion properties may instead reflect intrinsic regional differences in axon diameter, myelination, and fiber packing density across corpus callosum subregions. Thus, future studies should integrate DTI with histological or molecular assessments to directly

quantify axon diameter, myelin thickness, and fiber density of the corpus callosum following prolonged dietary SL intervention.

Collectively, diffusion MRI findings remain inconsistent across studies, with increases and decreases in diffusion-derived metrics reported across brain regions and developmental stages, while several studies have detected few or no significant effects. Heterogeneity in voxel resolution, developmental timing, diffusion acquisition protocols, and ROI definition further limits cross-study comparability and precludes the establishment of a consistent HMO-associated DTI signature.

### *3.7. Myelin Maturation in the Developing Brain Following Sialylated HMO Supplementation*

Myelin water fraction (MWF) has emerged as a robust, non-invasive biomarker for detecting regional changes in brain myelination [37]. Since the process of myelination underpins the formation of efficient neural circuits from infancy through adulthood [31], increased MWF values are widely interpreted as indicators of neurodevelopmental progress and cognitive potential [38]. In piglets supplemented with 6′-SL, elevated MWF was observed in the left hippocampus—a region known to undergo prolonged myelination during development [39]—suggesting that 6′-SL may promote region-specific myelin maturation. Likewise, higher MWF values were detected in the left superior colliculus of 3′-SL-supplemented pigs, a structure integral to visuomotor integration [40]. Although these increases were confined to a single hemisphere, previous work in primates has reported asymmetric Sia distribution within the brain, with higher concentrations in the left hemisphere [26], raising the possibility of asymmetric HMO-mediated myelination effects.

### *3.8. Metabolic Signatures of HMO Supplementation Revealed by MRS*

Magnetic resonance spectroscopy (MRS) studies have reported mixed results on the effects of HMO supplementation on brain metabolites and neurotransmitter profiles in piglets. Despite administering varying SL concentrations (130–760 mg/L) for approximately 30 days, Mudd et al. (2017) reported no significant differences in brain metabolite profiles between supplemented and control groups [24]. Consistently, the administration of the fucosylated HMO—2′-FL—either alone or in combination with OF or BMOs, did not result in any significant alterations in global brain metabolic status [21,22]. On the contrary, Wang et al. (2019) demonstrated significant alteration of brain metabolite and neurotransmitter concentration, required for optimizing neurodevelopment, following supplementation with sialylated HMOs [23]. Specifically, supplementation with a combination of SL and 6′-SLN (SL/SLN) significantly elevated absolute and relative concentrations of Glu, mIn, and the combined Glu–Gln pool (Glx). Furthermore, several metabolites—including NAA, tNAA, total choline (tCho), total creatine (tCr), glutathione (GSH), and scyllo-inositol (SIns)—showed positive correlation with total white matter volume, suggesting a potential link between HMO-induced metabolic changes and structural brain development. More recently, the combined HMO and lactoferrin (Lf) supplementation was associated with differences in selected cerebral metabolite concentrations compared with the control and HMO-only groups, as assessed by short echo time MRS [18]. However, the absence of a Lf-only group precludes disentangling the independent effects of Lf from potential additive or synergistic effects of the combined supplementation. Co-supplementation with combined HMOs (cHMOs) and Lf resulted in significantly higher absolute levels of total lipids and macromolecules (tLM), along with increased relative concentrations of GSH, tCr, tCho, and tLM. cHMOs alone showed a similar upward trend in tCr, tCho, and tLM and had significantly higher absolute tNAA levels than the other groups. The observed differences in MRS-derived metabolite concentrations indicate changes in regional brain neurochemical profiles following HMO-containing dietary interventions. Although these

metabolites are involved in lipid mobilization, energy homeostasis, antioxidant defense, neuronal integrity, and membrane turnover, changes in their concentrations do not necessarily indicate improved neuronal integrity, synaptic function, or neurodevelopment. Such interpretations require validation through complementary functional, histological, and molecular assessments [18].

The variability in MRS findings across studies likely reflects differences in experimental design and methodological implementation—particularly with respect to HMO composition, dosage, and timing of HMO supplementation. Amin et al. (2026) and Wang et al. (2019) administered a relatively high concentration of HMOs (3′-SL, 6′-SL, and 2′-FL at 1800 mg/L; 3′-SL and 6′-SL at 1710 mg/L, respectively), whereas Mudd et al. (2017) used a bovine-derived whey protein formulation enriched with lower levels of mixed SL (130–760 mg/L) [18,23,24]. Notably, the experimental diets used by Mudd et al. (2017) [24] contained DHA (174 mg/L), ARA (348 mg/L), GOS (2 g/L), and PDX (2 g/L) at comparable concentrations in both control and SL-supplemented groups. Although these shared dietary components are unlikely to independently confound within-study treatment comparisons, they may influence the background neurodevelopmental environment and potentially modify responses to SL supplementation. However, such interactions were not directly investigated. Furthermore, differences in background nutritional formulations across studies may contribute to the heterogeneity of MRS findings and limit direct comparisons of HMO-associated neurometabolic outcomes.

In studies focusing on fucosylated HMOs, Fleming et al. (2020) [21,22] supplemented piglets with 2′-FL (1 g/L), either alone or in combination with LNnT (0.5 g/L). Notably, these 2′-FL concentrations are substantially lower than those naturally found in human colostrum or mature milk (2.28–3.18 g/L [6]). Differences in the timing of MRS acquisition may have further contributed to inconsistent findings across studies. Fleming et al. (2020) and Mudd et al. (2017) performed MRS scans at PND 32–33, whereas Amin et al. (2026) and Wang et al. (2019) conducted metabolic assessments at PND 38/39 [18,21–24]. Based on whole-brain volume data, Conrad and Johnson (2015) estimated that one postnatal week in pigs corresponds approximately to one month of human brain development, highlighting that these seemingly modest differences in acquisition timing may correspond to meaningful developmental differences [41]. Additional methodological heterogeneity was evident across studies, including variations in MRS pulse sequences, echo time, voxel placement, and metabolite quantification approaches. Collectively, these methodological nuances underscore the need for greater harmonization of HMO dosage, supplementation duration, MRS acquisition parameters, and quantification strategies—to enable more robust interpretation and cross-study comparisons in future investigations of HMO-related neurodevelopmental effects.

### *3.9. Overall Interpretation of Neuroimaging*

Collectively, the available preclinical neuroimaging studies suggest heterogeneous and predominantly region-specific responses to HMO-containing interventions, with no consistent evidence of improved brain development. Structural MRI studies have generally reported no significant effects on global brain volume, although isolated regional volumetric differences have been observed. DTI findings are similarly inconsistent, with both increases and decreases in diffusion-derived metrics reported across brain regions and developmental stages. Myelin-sensitive imaging has identified differences in selected regions, while MRS studies have reported alterations in specific cerebral metabolites following certain HMO formulations; however, null findings have also been reported. Importantly, these neuroimaging findings do not establish enhanced neuronal maturation, myelination, or cognitive function, as their functional significance remains uncertain without complementary functional and

molecular validation. Differences in HMO composition, dosage, developmental timing, comparator diets, imaging protocols, and methodological quality further limit cross-study comparability. Therefore, the evidence supports the possibility that HMO-containing interventions influence aspects of brain structure, microstructure, and metabolism, but does not yet establish a beneficial effect on neurodevelopment.

### *3.10. Potential Mechanisms Linking Sialylated HMOs to Neuroimaging Markers of Brain Development*

Emerging preclinical evidence suggests that sialylated HMOs may influence molecular and cellular pathways involved in brain development, including myelination, ganglioside biosynthesis, sialic acid metabolism, glutamatergic signaling, and glial function [42]. However, the molecular observations and neuroimaging findings discussed in this review have largely been derived from independent investigations involving different HMO formulations, dosages, developmental stages, and experimental conditions. Although these findings provide biological plausibility for potential HMO-associated neurodevelopmental effects, they do not establish direct mechanistic relationships between specific molecular pathways and the observed neuroimaging changes. Accordingly, the following sections discuss these pathways as potential explanatory mechanisms and identify priorities for future integrated molecular and neuroimaging investigations.

### *3.11. Myelination and White Matter Development*

Myelin water fraction (MWF)—a well-established neuroimaging biomarker reflecting myelin content within white matter [37]—was increased in the left hippocampus and left superior colliculus of SL-supplemented piglets [19], consistent with possible region-specific increases in myelin-associated tissue characteristics. Consistent with these imaging findings, SL supplementation upregulated key myelination-related genes in the hippocampus—including myelin-associated glycoprotein (MAG), myelin basic protein (MBP), and myelin oligodendrocyte glycoprotein (MOG) [10]. These independent findings suggest a potential association between SL supplementation and myelin-related processes, although the underlying mechanisms remain unclear [10]. Such increases in myelin content are expected to reduce DTI metrics, such as mean diffusivity (MD) and radial diffusivity (RD), across maturing white matter regions, including the cerebellum, hippocampus, and corpus callosum [19,24], as progressive axonal ensheathment increasingly restricts water diffusion. By promoting myelin accumulation and white matter maturation, sialylated HMOs may support the development of coherent neural connectivity, essential for cognitive and motor development during early life. Although independent studies have reported alterations in myelination-related gene expression and regional myelin-sensitive neuroimaging measures following sialylated HMO supplementation, these findings do not establish a causal mechanistic link. Nevertheless, they support a plausible association between sialylated HMOs and myelin-related processes, warranting further investigation through integrated molecular, histological, and neuroimaging approaches.

### *3.12. Sialic Acid (Sia) Metabolism and Ganglioside Biosynthesis*

SL supplementation upregulated genes involved in Sia metabolism, including NEU1, encoding neuraminidase-1, and SLC17A5, encoding the lysosomal Sia transporter sialin [10]. These changes suggest enhanced intracellular trafficking, recycling, and availability of free Sia for downstream biosynthetic pathways [43]. In addition, SL intervention increased expression of ST8Sia IV, a key polysialyltransferase responsible for the synthesis of polySia on neural cell adhesion molecules (polySia-NCAMs), which play critical roles in neuronal plasticity, migration, and synaptic remodeling during brain development [12,44,45]. In

parallel, genes involved in ganglioside biosynthesis, including B3GALT4, encoding beta-1,3-galactosyltransferase 4, were upregulated [10], indicating an increased capacity for the synthesis of sialylated glycolipids in the developing brain [45,46].

Sialic acid (Sia), a family of nine-carbon monosaccharide abundant in sialylated HMOs, is a critical component of brain gangliosides and sialylated glycoproteins [45]. These sialylated molecules are essential for neuronal membrane stability, cell–cell interactions, and signal transduction [46]. They contribute to synapse formation and plasticity by influencing dendritic arborization, axonal growth, and neurogenesis [12]. In particular, polySia-NCAM is a key regulator of neuronal migration, synaptic plasticity, and circuit refinement, thereby supporting region-specific brain growth during development [46,47]. Consistent with these mechanisms, experimental studies in animal models indicate that dietary supplementation with sialylated HMOs enhances brain Sia content [48], increases synaptic plasticity [49], and promotes hippocampal neurogenesis [50], while also modulating developmental gene programs in the prefrontal cortex [51]. At the tissue level, these molecular effects may contribute to regional structural changes in the pons, cerebral aqueduct, or midbrain, potentially detectable using MRI-based volumetric measures. In parallel, DTI provides complementary sensitivity to microstructural refinement, reflected by increased fractional anisotropy and enhanced white matter tract coherence that may accompany regional brain growth and maturation. However, whether such alterations contribute to the regional volumetric or microstructural differences identified through neuroimaging remains uncertain, as direct associations between these molecular pathways and imaging outcomes have not been established.

### *3.13. Brain Metabolites and Neurotransmitters*

Sialylated HMOs (e.g., SL/SLN) have been associated with alterations in neuronal- and glial-related neurochemical profiles. SL/SLN supplementation was associated with increased absolute and relative concentrations of glutamate, glutamate–glutamine (Glx), and myo-inositol, alongside upregulated hippocampal expression of GRIN1, which encodes the obligatory GluN1 subunit of the NMDA receptor [22]. Increased GRIN1 expression may influence NMDA receptor-mediated glutamatergic signaling and synaptic responsiveness, providing a plausible hypothesis for the observed elevations in glutamate and Glx. However, as these molecular and metabolic findings derive from independent investigations, a direct mechanistic link between GRIN1 expression and MRS-derived metabolite changes has not been established [52]. The mechanisms underlying SL supplementation-associated increases in brain myo-inositol remain incompletely understood but may involve astrocyte-mediated pathways. SL supplementation has been shown to upregulate glial fibrillary acidic protein (GFAP), a canonical marker of astrocyte activation, which correlates strongly with elevated myo-inositol levels in the brain, consistent with astrocytic metabolic and osmotic activity [53]. These independent molecular and metabolic findings suggest potential involvement of neuronal and glial pathways, although their coordinated modulation has not been directly demonstrated.

Collectively, the available molecular and cellular evidence provides a biologically plausible framework for interpreting selected neuroimaging findings associated with HMO supplementation. However, these observations do not establish that the proposed pathways directly mediate the reported structural, microstructural, or metabolic changes. Further studies integrating molecular analyses with multimodal neuroimaging and functional assessments under comparable experimental conditions are required to investigate these potential mechanistic relationships. Nevertheless, these convergent findings provide a mechanistic framework for generating hypotheses about the relationship between early-life sialylated HMO exposure and neuroimaging markers of brain structure and function.

The potential mechanisms linking sialylated HMOs to neuroimaging markers of brain development are summarized in Figure 4.

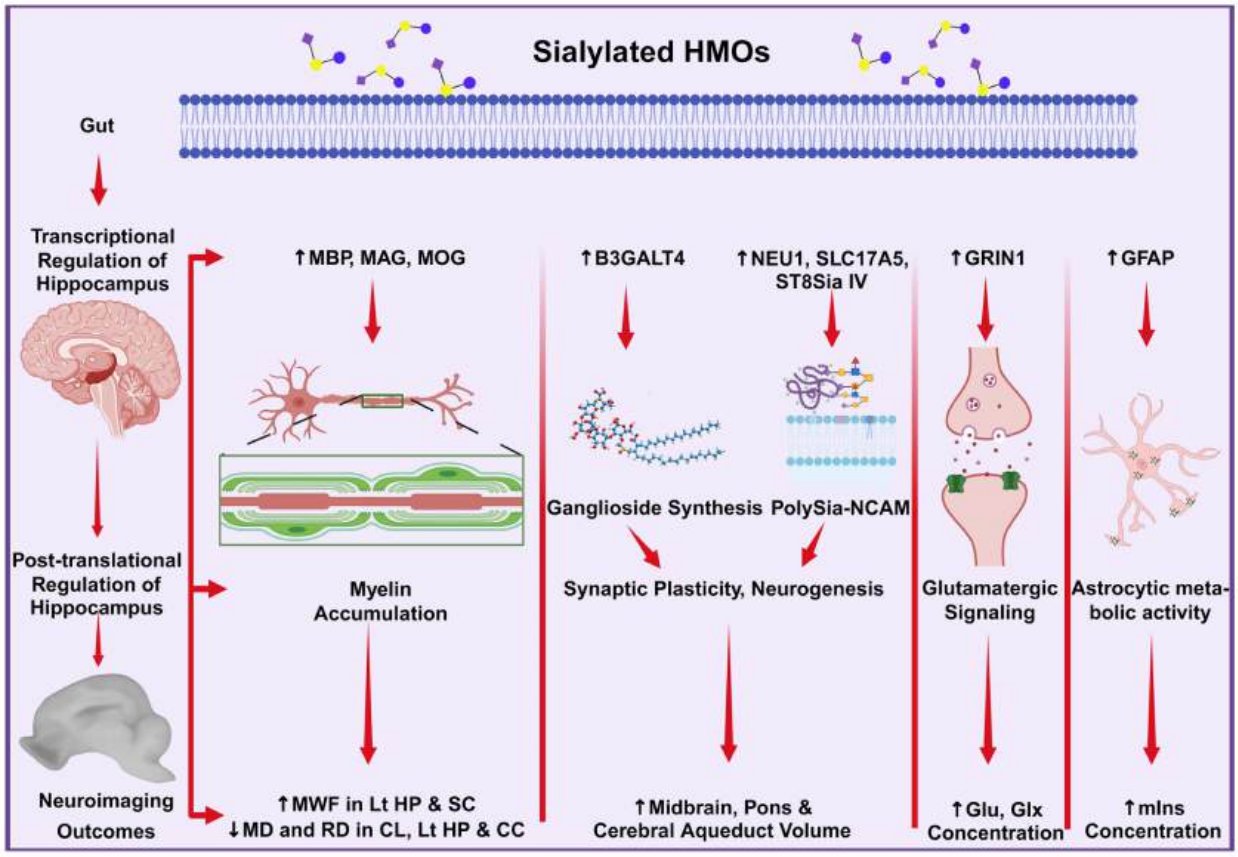



**Figure 4.** Potential mechanisms linking sialylated HMOs to neuroimaging markers of brain development. Exogenous sialylated HMOs (e.g., sialyllactose) are absorbed through the gastrointestinal tract and upregulate the expression of genes involved in myelination (MBP, MAG, and MOG), ganglioside biosynthesis (B3GALT4), sialic acid metabolism (NEU1, SLC17A5, and ST8Sia IV), glutamatergic signaling (GRIN1), and astrocytic function (GFAP). These molecular changes may correspond to increased white matter integrity (↑ MWF, ↓ MD, and RD), structural maturation of the pons, midbrain, and cerebral aqueduct, and elevated concentrations of Glu, Glx, and mIns, as measured by neuroimaging. Abbreviations: myelin basic protein (MBP); myelin-associated glycoprotein (MAG); myelin oligodendrocyte glycoprotein (MOG); myelin water fraction (MWF); left hippocampus (Lt HP); superior colliculus (SC); mean diffusivity (MD); radial diffusivity (RD); cerebellum (CL); corpus callosum (CC); beta-1,3-galactosyltransferase 4 (B3GALT4); neuraminidase-1 (NEU1); solute carrier family 17 member 5 (SLC17A5); ST8 alpha-N-acetyl-neuraminide alpha-2,8-sialyltransferase 4 (ST8Sia IV); polysialic acid (polySia); neural cell adhesion molecule (NCAM); glutamate ionotropic receptor NMDA type subunit 1 (GRIN1); glutamate (Glu); glutamate + glutamine (Glx); glial fibrillary acidic protein (GFAP); myo-inositol (mIns).

### *3.14. Potential Mechanisms Linking Fucosylated HMOs to Neuroimaging Markers of Brain Development*

Emerging evidence suggests that fucosylated HMOs influence neuronal growth, synaptic maturation, and network formation [54,55], with effects that can be detected using neuroimaging modalities. Supplementation with 2′-FL has been associated with increased relative volumes of the olfactory bulbs and pons [20,21], indicating region-specific structural brain differences. These structural differences may arise indirectly through the prebiotic actions of 2′-FL on the gut microbiota, including enrichment of Lactobacillus and Bacteroides taxa and the consequent elevation of microbially derived SCFAs. SCFAs, including acetate,

have been implicated in the regulation of central nervous system (CNS) development via modulation of neurotrophic signaling pathways, including enhanced expression of brain-derived neurotrophic factor (BDNF) within the hippocampus and frontal cortex [56]. Experimental evidence further indicates that SCFAs promote neuronal plasticity, stimulate hippocampal neurogenesis, and support dendritic growth and synaptogenesis [57,58], providing a plausible mechanistic link between early 2′-FL exposure and region-specific brain maturation.

Preclinical studies indicate that fucosylated HMOs, particularly 2′-FL, exert direct effects on neuronal development and synaptic plasticity. In rodent and piglet models, dietary 2′-FL supplementation enhances learning and memory [54,55] and is accompanied by molecular changes consistent with increased synaptic plasticity, including upregulation of neurotrophic signaling pathways, such as BDNF [54]. At the synaptic level, 2-FL has been associated with increased hippocampal long-term potentiation and enhanced expression of plasticity-related genes, supporting maturation of hippocampal and cortical circuits involved in cognition [54]. These molecular and cellular findings provide biologically plausible mechanisms that may help explain neuroimaging differences reported in independent studies. Whether these proposed molecular pathways contribute to regional structural or microstructural differences detected by MRI and DTI remains to be determined. Collectively, these findings suggest that fucosylated HMOs may support brain maturation through both indirect gut-mediated pathways and direct neurodevelopmental mechanisms, with corresponding neuroimaging markers reflecting structural and microstructural brain changes (Figure 5). Longitudinal studies integrating detailed HMO profiling with multimodal neuroimaging will be essential to establish causality and identify sensitive windows of exposure.

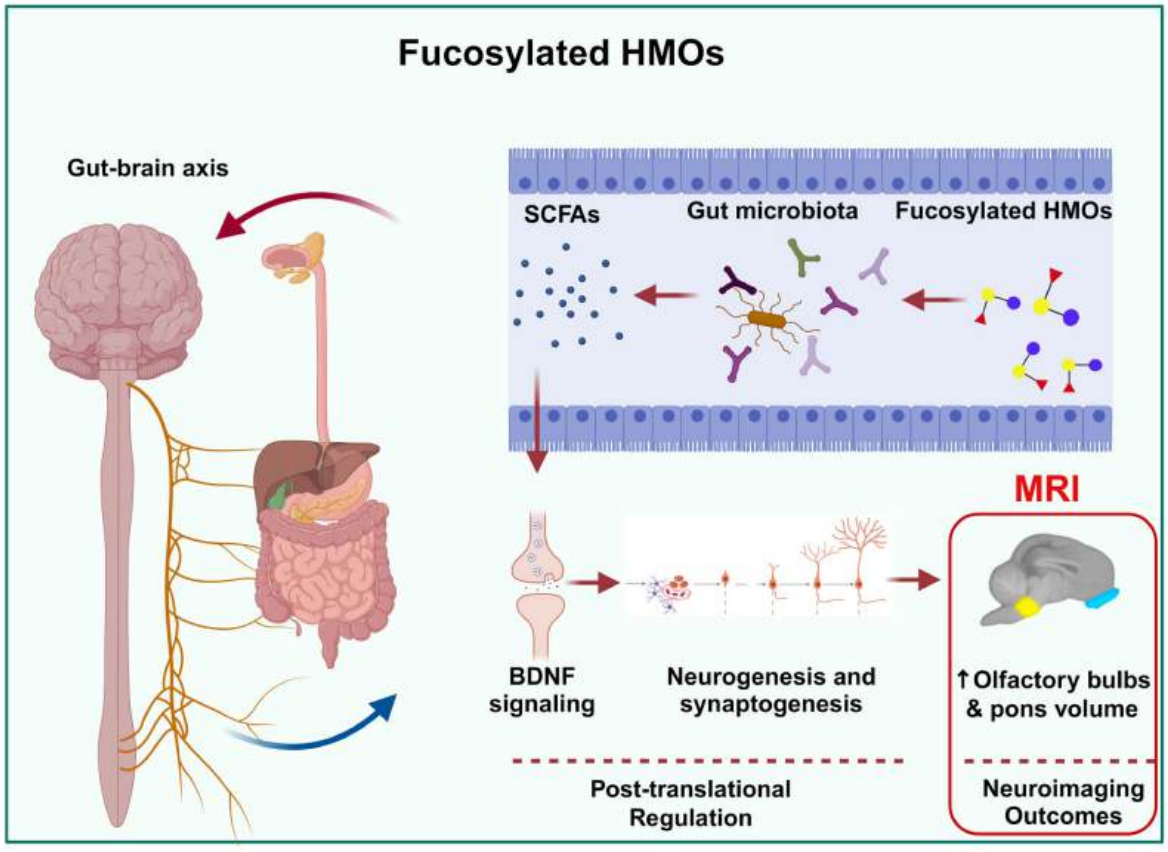



**Figure 5.** Potential mechanisms linking fucosylated HMOs to neuroimaging markers of brain development. Exogenous fucosylated HMOs may support brain maturation through both indirect

and direct mechanisms. Indirectly, they modulate the gut microbiota, alter metabolite profiles, and enhance the production of short-chain fatty acids (SCFAs), which in turn influence brain development. Directly, fucosylated HMOs can upregulate neurotrophic signaling pathways, including brain-derived neurotrophic factor (BDNF), thereby promoting neuronal growth and connectivity. Collectively, these processes facilitate neurogenesis, synaptogenesis, and microstructural refinement, leading to region-specific brain growth detectable by neuroimaging, including increased volumes of the pons and olfactory bulbs. MRI: magnetic resonance imaging.

### *3.15. Clinical Translation of Piglet Models*

The neonatal piglet offers a highly translational preclinical platform for investigating how early-life nutrition, including HMOs, influences brain development. Similar to humans, pigs experience a pronounced brain growth spurt extending from late gestation through early postnatal life, and their gyrencephalic brains share key neuroanatomical features with human infants, including comparable gray and white matter distribution, cortical folding, and developmental trajectories of white matter maturation [35]. Importantly, the size of the piglet brain is well suited to clinical neuroimaging platforms, enabling the use of structural MRI and DTI with protocols analogous to those applied in human infants. In addition, the piglet's precocial development allows for early weaning, dietary manipulation, controlled HMO exposure at physiologically relevant doses, and integration of behavioral, molecular, and histological assessments. Together, these attributes position the piglets as a powerful translational bridge between mechanistic studies and clinical neuroimaging, allowing identification of plausible neurodevelopmental pathways, dose–response relationships, and imaging biomarkers that can inform future human trials [41]. Despite its translational relevance, the neonatal piglet model presents anatomical, developmental, and experimental limitations that constrain extrapolation to human infants. Although the porcine and human brain share several neuroanatomical characteristics, notable interspecies differences remain. While subcortical structures are relatively well characterized in pigs [59], the neocortex lacks a comprehensive cytoarchitectonic and functional mapping framework equivalent to the human Brodmann areas [60]. Interspecies differences in brain maturation, developmental trajectories, gastrointestinal physiology, and dietary HMO exposure may further influence responses to HMO supplementation. Moreover, artificial rearing, standardized feeding regimens, and variations in HMO composition and dosage may not adequately reflect the complex nutritional and environmental exposures of human infants. Consequently, changes in regional brain volumes, diffusion-derived metrics, or cerebral metabolite concentrations in piglets cannot be assumed to translate into improved neurodevelopmental outcomes in humans. Given the heterogeneity of the preclinical evidence and the absence of eligible human intervention studies incorporating neuroimaging outcomes, current findings remain preliminary and hypothesis-generating. Well-designed longitudinal human intervention studies integrating multimodal neuroimaging with cognitive, behavioral, and molecular assessments are needed to establish the neurodevelopmental significance and clinical relevance of HMO supplementation.

### *3.16. Limitations of Neuroimaging-Based HMO Research*

Despite growing interest in HMOs, interventional studies linking HMO exposure to neuroimaging outcomes remain scarce in both human infants and rodent models. Historically, HMO research has prioritized gastrointestinal and immune outcomes, with neurodevelopmental endpoints receiving attention only recently [61]. In human infants, ethical and logistical constraints—such as the need for specialized infrastructure and in some cases, sedation—have limited the feasibility of incorporating MRI into nutritional intervention trials. To date, only a single cross-sectional observational study has examined associations between HMO exposure and infant brain tissue organization using MRI [58]. Conducted in

a cohort of Hispanic infants from Los Angeles, California, this study reported differential associations between fucosylated and sialylated HMOs and voxel-wise measures of brain microstructure and regional cerebral blood flow [58]. Higher exposure to 3′-FL and 3′-SL was associated with increased fractional anisotropy, reduced mean diffusivity, and elevated regional cerebral blood flow in developing white matter, whereas 2′-FL exposure was linked to reduced fractional anisotropy, increased mean diffusivity, and lower cerebral blood flow in the cortical mantle. Exposure to 6′-SL showed no significant associations. However, the cross-sectional design and single time-point assessment of both HMO exposure and neuroimaging outcomes limit causal inference, highlighting the need for longitudinal and interventional studies. Comparable feasibility and cost constraints have limited the use of nonhuman primate models. Rodent models, while widely employed in nutritional neuroscience, have limited translational relevance due to fundamental differences in brain morphology, developmental timing, and white matter organization compared with humans [41]. Together, these factors contribute to the current paucity of neuroimaging-based HMO research in both clinical and rodent-based preclinical settings.

Research has also been biased toward fucosylated HMOs, partly due to historical challenges in accessing food-grade sialylated structures [5]. Among sialylated HMOs, 3′-SL has been more frequently studied and at higher concentrations than 6′-SL [23], despite 6′-SL being more abundant in human breast milk [62,63]. Experimental designs also lack ecological validity, as most studies assess individual HMOs in isolation, rather than the complex mixtures present in human milk. This limitation underscores the need to evaluate combined formulations—particularly blends of fucosylated and sialylated HMOs—to more accurately capture the functional complexity of human milk in preclinical models.

A persistent challenge in study design is the selection of appropriate control diets. Lactose, frequently employed as a control carbohydrate, differs fundamentally from HMOs in digestibility and metabolic fate. Rigorous studies should, therefore, use control diets devoid of sialylated and fucosylated structures and matched in fiber load using non-fermentable, microbiota-inert agents, such as methylcellulose.

Methodological challenges in preclinical neuroimaging also limit progress. Accurate brain extraction remains difficult, as widely used tools—FSL-BET, ANTs, ITK-SNAP, and 3D Slicer—are optimized for human neuroanatomy and often fail to generalize to species like pigs. While algorithms such as Veterinary Images Brain Extraction (VIBE) show promise in canine and feline species [64], results in piglets remain suboptimal, necessitating labor-intensive manual extraction prone to operator bias. In addition, age-specific MRI atlases exist only for four- and eight-week-old piglets, leaving other critical developmental windows underrepresented and limiting temporal resolution. Finally, variability in scan timing, acquisition parameters, and quantification strategies further impedes cross-study comparability.

An important limitation of the current neuroimaging evidence base is its reliance on neonatal piglet models. Although piglets provide valuable neurodevelopmental and neuroanatomical advantages for translational neuroimaging, findings from a single preclinical species cannot be directly extrapolated to human infants. Moreover, human neuroimaging evidence remains extremely limited, precluding robust conclusions regarding the causal effects or clinical efficacy of HMO supplementation on brain development.

## 4. Limitations of Review Process

Several methodological considerations should be acknowledged. Strengths of the review process included independent study selection, data extraction, and risk-of-bias assessment by two reviewers, as well as a formal risk-of-bias evaluation of all included animal intervention studies using SYRCLE's tool. Nevertheless, the literature search was restricted to three bibliographic databases, and reference lists were not systematically screened. In

addition, the review was not preregistered, and formal assessments of reporting bias and certainty of evidence at the synthesis level were not undertaken. These considerations should be taken into account when interpreting the findings.

## 5. Future Directions

Neuroimaging-based HMO research remains in its infancy. Elucidating the full neurodevelopmental potential of HMOs will require longitudinal preclinical studies with harmonized methodologies, complemented by carefully designed clinical trials. Integrating neuroimaging with histological and molecular analyses will enable the mapping of HMO-driven adaptations across cellular- to systems-level scales.

Given the compositional complexity of human milk, future work should move beyond single-molecule approaches to evaluate combined HMO formulations—particularly blends of fucosylated and sialylated HMOs—to better capture biologically relevant interactions. Rigorously controlled diets—including the use of non-fermentable fiber substitutes such as methyl cellulose—are essential to disentangle microbiome-mediated effects from HMO-specific effects.

Existing preclinical findings provide candidate imaging biomarkers and methodological guidance for future human studies. Prospective longitudinal studies and adequately powered randomized controlled trials should evaluate well-characterized HMO formulations at physiologically relevant doses, using harmonized MRI acquisition and analytical protocols, and integrating neuroimaging outcomes with validated behavioral and developmental assessments. Such studies are essential to determine whether neuroimaging changes associated with HMO exposure in preclinical models translate into clinically meaningful neurodevelopmental benefits in human infants.

Finally, harmonization of experimental parameters—including HMO dose, imaging modality, metabolite acquisition site, sequence selection, and quantification strategy—will be critical for robust cross-study comparisons. Realizing the neurodevelopmental potential of HMOs will ultimately require interdisciplinary strategies integrating nutritional neuroscience, advanced imaging, and systems-level biology.

**Supplementary Materials:** The following supporting information can be downloaded at: https://www.mdpi.com/article/10.3390/nu18223869/s1. Table S1: Complete database-specific search strategies for PubMed, Scopus, and Ovid MEDLINE, including search terms, search restrictions, and reporting details in accordance with PRISMA-S; Table S2: SYRCLE risk-of-bias assessment of the eight included studies, presenting judgments across ten methodological domains with study-specific supporting evidence and justifications; Table S3: Completed PRISMA 2020 checklist indicating the locations of the corresponding reporting items in the manuscript [65].

**Author Contributions:** M.M.A., conceptualization, data curation, methodology, writing—original draft, writing—review and editing; T.A., visualization, writing—review and editing, methodology, data curation; A.A.D.I.A., writing—review and editing, data curation; X.Z., writing—review and editing; Z.Z., writing—review and editing; B.W., conceptualization, supervision, validation, funding acquisition, writing—review and editing, and final approval of the manuscript for submission. All authors have read and agreed to the published version of the manuscript.

**Funding:** M.M.A. was supported by the PhD Scholarships in Neuroimaging (project No. 103878), and A.A.D.I.A was supported by the PhD Scholarship in Animal Behaviour and Molecular Nutrition (project No. 103878), both awarded by Charles Sturt University through the Gulbali Institute, Australia. T.A. was supported by the 2024 Gulbali Institute PhD Scholarship awarded by Charles Sturt University, Australia.

**Data Availability Statement:** All data supporting the findings of this systematic review were obtained from previously published studies. The extracted study characteristics, neuroimaging findings, and methodological details are presented in Tables 2 and 3. The database-specific search strategies and study-level risk-of-bias assessments are provided in Supplementary Tables S1 and S2, respectively. No meta-analysis was performed; therefore, no statistical synthesis code was generated. No additional datasets or data extraction templates are publicly available.

**Conflicts of Interest:** The authors declare no conflicts of interest.

## References


1. Kim, S.Y.; Yi, D.Y. Components of human breast milk: From macronutrient to microbiome and microRNA. *Clin. Exp. Pediatr.* **2020**, *63*, 301–309. [CrossRef] [PubMed]
2. Urashima, T.; Asakuma, S.; Leo, F.; Fukuda, K.; Messer, M.; Oftedal, O.T. The predominance of type I oligosaccharides is a feature specific to human breast milk. *Adv. Nutr.* **2012**, *3*, 473S–482S. [CrossRef] [PubMed]
3. Wei, J.; Wang, Z.A.; Wang, B.; Jahan, M.; Wang, Z.; Wynn, P.C.; Du, Y. Characterization of porcine milk oligosaccharides over lactation between primiparous and multiparous female pigs. *Sci. Rep.* **2018**, *8*, 4688. [CrossRef] [PubMed]
4. Vandenplas, Y.; Berger, B.; Carnielli, V.P.; Ksiazyk, J.; Lagstrom, H.; Luna, M.S.; Migacheva, N.; Mosselmans, J.; Picaud, J.; Possner, M.; et al. Human Milk Oligosaccharides: 2′-Fucosyllactose (2′-FL) and Lacto-N-Neotetraose (LNnT) in Infant Formula. *Nutrients* **2018**, *10*, 1161. [CrossRef] [PubMed]
5. Dinleyici, M.; Barbieur, J.; Dinleyici, E.C.; Vandenplas, Y. Functional effects of human milk oligosaccharides (HMOs). *Gut. Microbes* **2023**, *15*, 2186115. [CrossRef] [PubMed]
6. Soyyilmaz, B.; Miks, M.H.; Rohrig, C.H.; Matwiejuk, M.; Meszaros-Matwiejuk, A.; Vigsnaes, L.K. The Mean of Milk: A Review of Human Milk Oligosaccharide Concentrations throughout Lactation. *Nutrients* **2021**, *13*, 2737. [CrossRef] [PubMed]
7. Walsh, C.; Lane, J.A.; van Sinderen, D.; Hickey, R.M. Human milk oligosaccharides: Shaping the infant gut microbiota and supporting health. *J. Funct. Foods* **2020**, *72*, 104074. [CrossRef] [PubMed]
8. Zhu, L.; Wang, M.; Li, H.; Luo, T.; Deng, Z.; Li, J.; Zheng, L.; Zhang, B. Supplementation of 3′-Sialyllactose During the Growth Period Improves Learning and Memory Development in Mice. *J. Agric. Food Chem.* **2024**, *72*, 24518–24529. [CrossRef] [PubMed]
9. Abdul Khalid, S.K.; Rashed, A.A.; Aziz, S.A.; Ahmad, H. Effects of sialic acid from edible bird nest on cell viability associated with brain cognitive performance in mice. *World J. Tradit. Chin. Med.* **2019**, *5*, 214–219. [CrossRef] [PubMed]
10. Obelitz-Ryom, K.; Bering, S.B.; Overgaard, S.H.; Eskildsen, S.F.; Ringgaard, S.; Olesen, J.L.; Skovgaard, K.; Pankratova, S.; Wang, B.; Brunse, A.; et al. Bovine milk oligosaccharides with sialyllactose improves cognition in preterm pigs. *Nutrients* **2019**, *11*, 1335. [CrossRef] [PubMed]
11. Wang, B.; Yu, B.; Karim, M.; Hu, H.; Sun, Y.; McGreevy, P.; Petocz, P.; Held, S.; Brand-Miller, J. Dietary sialic acid supplementation improves learning and memory in piglets. *Am. J. Clin. Nutr.* **2007**, *85*, 561–569. [CrossRef] [PubMed]
12. Wang, B. Sialic acid is an essential nutrient for brain development and cognition. *Annu. Rev. Nutr.* **2009**, *29*, 177–222. [CrossRef] [PubMed]
13. Camacho, M.; Wilms, M.; Almgren, H.; Amador, K.; Camicioli, R.; Ismail, Z.; Monchi, O.; Forkert, N.D. Exploiting macro- and micro-structural brain changes for improved Parkinson's disease classification from MRI data. *npj Park. Dis.* **2024**, *10*, 43. [CrossRef] [PubMed]
14. Gujar, S.K.; Maheshwari, S.; Bjorkman-Burtscher, I.; Sundgren, P.C. Magnetic resonance spectroscopy. *J. Neuroophthalmol.* **2005**, *25*, 217–226. [CrossRef] [PubMed]
15. Fan, Y.; McMath, A.L.; Donovan, S.M. Review on the impact of milk oligosaccharides on the brain and neurocognitive development in early life. *Nutrients* **2023**, *15*, 3743. [CrossRef] [PubMed]
16. Xu, J.; Song, J.; Xu, H.; Li, Z.; Ding, M.; Qiao, D.; Zhang, B.; Li, B. Structural diversity, composition variation and neurodevelopmental-promoting effects of human milk oligosaccharides: A systematic review. *Carbohydr. Polym.* **2025**, *368*, 124229. [CrossRef] [PubMed]
17. Suryawan, A.; Chairunita; Darma, A. Human milk oligosaccharides, brain structure, and cognitive development in infants: A narrative review. *Biomol. Biomed.* **2026**, *ahead of print*. [CrossRef] [PubMed]
18. Amin, M.M.; Amin, T.; Adikari, A.A.D.I.; Zheng, X.; Chen, Z.; Wang, B. Synergistic action of human milk oligosaccharides and lactoferrin enhances neurodevelopment in piglets: Evidence from MRS based metabolic profiling. *Nutr. Neurosci.* **2026**, *29*, 1200–1212. [CrossRef] [PubMed]
19. Golden, R.K.; Sutkus, L.T.; Donovan, S.M.; Dilger, R.N. Dietary supplementation of 3′-sialyllactose or 6′-sialyllactose elicits minimal influence on cognitive and brain development in growing pigs. *Front. Behav. Neurosci.* **2023**, *17*, 1337897. [CrossRef] [PubMed]

20. Sutkus, L.T.; Joung, S.; Hirvonen, J.; Jensen, H.M.; Ouwehand, A.C.; Mukherjea, R.; Donovan, S.M.; Dilger, R.N. Influence of 2′-Fucosyllactose and *Bifidobacterium longum* subspecies *infantis* supplementation on cognitive and structural brain development in young pigs. *Front. Neurosci.* **2022**, *16*, 860368. [CrossRef] [PubMed]
21. Fleming, S.A.; Mudd, A.T.; Hauser, J.; Yan, J.; Metairon, S.; Steiner, P.; Donovan, S.M.; Dilger, R.N. Dietary oligofructose alone or in combination with 2′-Fucosyllactose differentially improves recognition memory and hippocampal mRNA expression. *Nutrients* **2020**, *12*, 2131. [CrossRef] [PubMed]
22. Fleming, S.A.; Mudd, A.T.; Hauser, J.; Yan, J.; Metairon, S.; Steiner, P.; Donovan, S.M.; Dilger, R.N. Human and bovine milk oligosaccharides elicit improved recognition memory concurrent with alterations in regional brain volumes and hippocampal mRNA expression. *Front. Neurosci.* **2020**, *14*, 770. [CrossRef] [PubMed]
23. Wang, H.X.; Chen, Y.; Haque, Z.; de Veer, M.; Egan, G.; Wang, B. Sialylated milk oligosaccharides alter neurotransmitters and brain metabolites in piglets: An in vivo magnetic resonance spectroscopic (MRS) study. *Nutr. Neurosci.* **2019**, *24*, 885–895. [CrossRef] [PubMed]
24. Mudd, A.T.; Fleming, S.A.; Labhart, B.; Chichlowski, M.; Berg, B.M.; Donovan, S.M.; Dilger, R.N. Dietary sialyllactose influences sialic acid concentrations in the prefrontal cortex and magnetic resonance imaging measures in corpus callosum of young pigs. *Nutrients* **2017**, *9*, 1297. [CrossRef] [PubMed]
25. Mudd, A.T.; Salcedo, J.; Alexander, L.S.; Johnson, S.K.; Getty, C.M.; Chichlowski, M.; Berg, B.M.; Barile, D.; Dilger, R.N. Porcine milk oligosaccharides and sialic acid concentrations vary throughout lactation. *Front. Nutr.* **2016**, *3*, 39. [CrossRef] [PubMed]
26. Wang, B.; Miller, J.B.; McNeil, Y.; McVeagh, P. Sialic acid concentration of brain gangliosides: Variation among eight mammalian species. *Comp. Biochem. Physiol. A Mol. Integr. Physiol.* **1998**, *119*, 435–439. [CrossRef] [PubMed]
27. Dobbing, J.; Sands, J. Quantitative growth and development of human brain. *Arch. Dis. Child.* **1973**, *48*, 757–767. [CrossRef] [PubMed]
28. Jelsing, J.; Nielsen, R.; Olsen, A.K.; Grand, N.; Hemmingsen, R.; Pakkenberg, B. The postnatal development of neocortical neurons and glial cells in the Gottingen minipig and the domestic pig brain. *J. Exp. Biol.* **2006**, *209*, 1454–1462. [CrossRef] [PubMed]
29. Carlson, S.E.; Colombo, J. Docosahexaenoic acid and arachidonic acid nutrition in early development. *Adv. Pediatr.* **2016**, *63*, 453–471. [CrossRef] [PubMed]
30. Fleming, S.A.; Monaikul, S.; Patsavas, A.J.; Waworuntu, R.V.; Berg, B.M.; Dilger, R.N. Dietary polydextrose and galactooligosaccharide increase exploratory behavior, improve recognition memory, and alter neurochemistry in the young pig. *Nutr. Neurosci.* **2019**, *22*, 499–512. [CrossRef] [PubMed]
31. Dubois, J.; Dehaene-Lambertz, G.; Kulikova, S.; Poupon, C.; Huppi, P.S.; Hertz-Pannier, L. The early development of brain white matter: A review of imaging studies in fetuses, newborns and infants. *Neuroscience* **2014**, *276*, 48–71. [CrossRef] [PubMed]
32. Alexander, A.L.; Lee, J.E.; Lazar, M.; Field, A.S. Diffusion tensor imaging of the brain. *Neurotherapeutics* **2007**, *4*, 316–329. [CrossRef] [PubMed]
33. Huppi, P.S.; Dubois, J. Diffusion tensor imaging of brain development. *Semin. Fetal. Neonatal. Med.* **2006**, *11*, 489–497. [CrossRef] [PubMed]
34. Barnea-Goraly, N.; Menon, V.; Eckert, M.; Tamm, L.; Bammer, R.; Karchemskiy, A.; Dant, C.C.; Reiss, A.L. White matter development during childhood and adolescence: A cross-sectional diffusion tensor imaging study. *Cereb. Cortex.* **2005**, *15*, 1848–1854. [CrossRef] [PubMed]
35. Conrad, M.S.; Dilger, R.N.; Johnson, R.W. Brain growth of the domestic pig (*Sus scrofa*) from 2 to 24 weeks of age: A longitudinal MRI study. *Dev. Neurosci.* **2012**, *34*, 291–298. [CrossRef] [PubMed]
36. Bennett, I.J.; Madden, D.J.; Vaidya, C.J.; Howard, D.V.; Howard, J.H., Jr. Age-related differences in multiple measures of white matter integrity: A diffusion tensor imaging study of healthy aging. *Hum. Brain Mapp.* **2010**, *31*, 378–390. [CrossRef] [PubMed]
37. Lee, J.; Hyun, J.W.; Lee, J.; Choi, E.J.; Shin, H.G.; Min, K.; Nam, Y.; Kim, H.J. So you want to image myelin using MRI: An overview and practical guide for myelin water imaging. *J. Magn. Reson. Imaging* **2021**, *53*, 360–373. [CrossRef] [PubMed]
38. Gibson, K.R. Myelination and behavioral development: A comparative perspective on questions of neoteny, altriciality and intelligence. In *Brain Maturation and Cognitive Development: Comparative and Cross-Cultural Perspectives*; Gibson, K.R., Petersen, A.C., Eds.; Aldine de Gruyter: Hawthorne, NY, USA, 1991; pp. 29–63.
39. Benes, F.M. Myelination of cortical-hippocampal relays during late adolescence. *Schizophr. Bull.* **1989**, *15*, 585–593. [CrossRef] [PubMed]
40. Zubricky, R.D.; Das, J.M. *Neuroanatomy, Superior Colliculus*; StatPearls Publishing: Treasure Island, FL, USA, 2024; pp. 1–6.
41. Conrad, M.S.; Johnson, R.W. The domestic piglet: An important model for investigating the neurodevelopmental consequences of early life insults. *Annu. Rev. Anim. Biosci.* **2015**, *3*, 245–264. [CrossRef] [PubMed]
42. Li, W.; Gunn, A.; Zheng, X.; Ma, J.; Sheng, N.; Wang, B. Exploring human milk oligosaccharides: Mechanisms linking gut function to cognitive development in human and pig physiology. *Front. Nutr.* **2025**, *12*, 1700954. [CrossRef] [PubMed]

43. Hobbs, M.; Jahan, M.; Ghorashi, S.A.; Wang, B. Current perspective of sialylated milk oligosaccharides in mammalian milk: Implications for brain and gut health of newborns. *Foods* **2021**, *10*, 473. [CrossRef] [PubMed]
44. Yang, C.; Zhang, P.; Fang, W.; Chen, Y.; Zhang, N.; Qiao, Z.; Troy, F.A.; Wang, B. Molecular mechanisms underlying how sialyllactose intervention promotes intestinal maturity by upregulating GDNF through a CREB-dependent pathway in neonatal piglets. *Mol. Neurobiol.* **2019**, *56*, 7994–8007. [CrossRef] [PubMed]
45. Wang, B. Molecular mechanism underlying sialic acid as an essential nutrient for brain development and cognition. *Adv. Nutr.* **2012**, *3*, 465S–472S. [CrossRef] [PubMed]
46. Schnaar, R.L.; Gerardy-Schahn, R.; Hildebrandt, H. Sialic acids in the brain: Gangliosides and polysialic acid in nervous system development, stability, disease, and regeneration. *Physiol. Rev.* **2014**, *94*, 461–518. [CrossRef] [PubMed]
47. Liu, F.; Simpson, A.B.; D'Costa, E.; Bunn, F.S.; van Leeuwen, S.S. Sialic acid, the secret gift for the brain. *Crit. Rev. Food Sci. Nutr.* **2022**, *63*, 9875–9894. [CrossRef] [PubMed]
48. Jacobi, S.K.; Yatsunenko, T.; Li, D.; Dasgupta, S.; Yu, R.K.; Berg, B.M.; Chichlowski, M.; Odle, J. Dietary isomers of sialyllactose increase ganglioside sialic acid concentrations in the corpus callosum and cerebellum and modulate the colonic microbiota of formula-fed piglets. *J. Nutr.* **2016**, *146*, 200–208. [CrossRef] [PubMed]
49. Pisa, E.; Martire, A.; Chiodi, V.; Traversa, A.; Caputo, V.; Hauser, J.; Macri, S. Exposure to 3′Sialyllactose-poor milk during lactation impairs cognitive capabilities in adulthood. *Nutrients* **2021**, *13*, 4191. [CrossRef]
50. Tarr, A.J.; Galley, J.D.; Fisher, S.E.; Chichlowski, M.; Berg, B.M.; Bailey, M.T. The prebiotics 3′Sialyllactose and 6′Sialyllactose diminish stressor-induced anxiety-like behavior and colonic microbiota alterations: Evidence for effects on the gut-brain axis. *Brain Behav. Immun.* **2015**, *50*, 166–177. [CrossRef] [PubMed]
51. Hauser, J.; Pisa, E.; Vasquez, A.A.; Tomasi, F.; Traversa, A.; Chiodi, V.; Martin, F.; Sprenger, N.; Lukjancenko, O.; Zollinger, A.; et al. Sialylated human milk oligosaccharides program cognitive development through a non-genomic transmission mode. *Mol. Psychiatry* **2021**, *26*, 2854–2871. [CrossRef] [PubMed]
52. Hasan, M.T.; Hernandez-Gonzalez, S.; Dogbevia, G.; Trevino, M.; Bertocchi, I.; Gruart, A.; Delgado-García, J.M. Role of motor cortex NMDA receptors in learning-dependent synaptic plasticity of behaving mice. *Nat. Commun.* **2013**, *4*, 2258. [CrossRef] [PubMed]
53. Hirata, K.; Matsuoka, K.; Tagai, K.; Endo, H.; Tatebe, H.; Ono, M.; Kokubo, N.; Kataoka, Y.; Oyama, A.; Shinotoh, H.; et al. In vivo assessment of astrocyte reactivity in patients with progressive supranuclear palsy. *Ann. Neurol.* **2024**, *96*, 247–261. [CrossRef] [PubMed]
54. Vazquez, E.; Barranco, A.; Ramirez, M.; Gruart, A.; Delgado-Garcia, J.M.; Martinez-Lara, E.; Blanco, S.; Martín, M.J.; Castanys, E.; Buck, R.; et al. Effects of a human milk oligosaccharide, 2′-fucosyllactose, on hippocampal long-term potentiation and learning capabilities in rodents. *J. Nutr. Biochem.* **2015**, *26*, 455–465. [CrossRef] [PubMed]
55. Oliveros, E.; Ramirez, M.; Vazquez, E.; Barranco, A.; Gruart, A.; Delgado-Garcia, J.M.; Buck, R.; Rueda, R.; Martin, M.J. Oral supplementation of 2′-fucosyllactose during lactation improves memory and learning in rats. *J. Nutr. Biochem.* **2016**, *31*, 20–27. [CrossRef] [PubMed]
56. Church, J.S.; Bannish, J.A.M.; Adrian, L.A.; Martinez, K.R.; Henshaw, A.; Schwartzer, J.J. Serum short chain fatty acids mediate hippocampal BDNF and correlate with decreasing neuroinflammation following high pectin fiber diet in mice. *Front. Neurosci.* **2023**, *17*, 1134080. [CrossRef] [PubMed]
57. Marrocco, F.; Carpini, M.D.; Garofalo, S.; Giampaoli, O.; De Felice, E.; Di Castro, M.A.; Maggi, L.; Scavizzi, F.; Raspa, M.; Marini, F.; et al. Short-chain fatty acids promote the effect of environmental signals on the gut microbiome and metabolome in mice. *Commun. Biol.* **2022**, *5*, 517. [CrossRef] [PubMed]
58. Berger, P.K.; Bansal, R.; Sawardekar, S.; Yonemitsu, C.; Furst, A.; Hampson, H.E.; Schmidt, K.A.; Alderete, T.L.; Bode, L.; Goran, M.I.; et al. Associations of human milk oligosaccharides with infant brain tissue organization and regional blood flow at 1 month of age. *Nutrients* **2022**, *14*, 3820. [CrossRef] [PubMed]
59. Felix, B.; Leger, M.E.; Albe-Fessard, D.; Marcilloux, J.C.; Rampin, O.; Laplace, J.P. Stereotaxic atlas of the pig brain. *Brain Res. Bull.* **1999**, *49*, 1–137. [CrossRef] [PubMed]
60. Sauleau, P.; Lapouble, E.; Val-Laillet, D.; Malbert, C.H. The pig model in brain imaging and neurosurgery. *Animal* **2009**, *3*, 1138–1151. [CrossRef] [PubMed]
61. Bode, L. Human milk oligosaccharides: Every baby needs a sugar mama. *Glycobiology* **2012**, *22*, 1147–1162. [CrossRef] [PubMed]
62. Zhou, Y.; Sun, H.; Li, K.; Zheng, C.; Ju, M.; Lyu, Y.; Zhao, R.; Wang, W.; Zhang, W.; Xu, Y.; et al. Dynamic changes in human milk oligosaccharides in Chinese population: A systematic review and meta-analysis. *Nutrients* **2021**, *13*, 2912. [CrossRef] [PubMed]
63. Thurl, S.; Munzert, M.; Boehm, G.; Matthews, C.; Stahl, B. Systematic review of the concentrations of oligosaccharides in human milk. *Nutr. Rev.* **2017**, *75*, 920–933. [CrossRef] [PubMed]

64. Eddin, J.N.; Dorez, H.; Curcio, V. Automatic brain extraction and brain tissues segmentation on multi-contrast animal MRI. *Sci. Rep.* **2023**, *13*, 6416. [CrossRef] [PubMed]
65. Page, M.J.; McKenzie, J.E.; Bossuyt, P.M.; Boutron, I.; Hoffmann, T.C.; Mulrow, C.D.; Shamseer, L.; Tetzlaff, J.M.; Akl, E.A.; Brennan, S.E.; et al. The PRISMA 2020 statement: An updated guideline for reporting systematic reviews. *BMJ* **2021**, *372*, n71. [CrossRef] [PubMed]

**Disclaimer/Publisher's Note:** The statements, opinions and data contained in all publications are solely those of the individual author(s) and contributor(s) and not of MDPI and/or the editor(s). MDPI and/or the editor(s) disclaim responsibility for any injury to people or property resulting from any ideas, methods, instructions or products referred to in the content.